

RESEARCH

Open Access



# Taxonomic, genomic, and ecological insights into a novel *Flavobacteriaceae* strain from coastal tidal flats

Haohao Wang<sup>1</sup>, Jiahui Liu<sup>1</sup>, Yifan Guo<sup>1</sup>, Yaqin Chen<sup>1</sup>, Chi Zhang<sup>1</sup>, Shan He<sup>2,3</sup>, Weiyan Zhang<sup>2\*</sup> and Lijian Ding<sup>2\*</sup>

## Abstract

**Background** Tidal flats are vital coastal ecosystems that play a significant role in organic carbon accumulation and biogeochemical cycles. Members of the family *Flavobacteriaceae* is known for its ability to degrade complex organic matter, including polysaccharides. However, the ecological roles and metabolic capabilities of *Flavobacteriaceae* in tidal flat environments remain underexplored.

**Results** In this study, we isolated and characterized a novel bacterium, strain NBU2967<sup>T</sup>, from the tidal flats of Meishan Island in the East China Sea. Phylogenetic and genomic analyses identified this strain as a new genus and species within the family *Flavobacteriaceae*, for which we propose the name *Meishania litoralis* gen. nov., sp. nov. Comprehensive polyphasic characterization, including morphological, physiological, chemotaxonomic, and genomic analyses, confirmed its distinct taxonomic status. Genomic analysis revealed a diverse set of carbohydrate-active enzymes (CAZymes), along with multiple metabolic pathways associated with carbon and sulfur cycling, highlighting the strain's potential adaptation to organic-rich marine environments. Comparative genomic and pangenome analyses further demonstrated significant genetic divergence from related taxa. Environmental distribution data revealed that the newly proposed genus *Meishania* is widely distributed across global marine ecosystems.

**Conclusions** We isolated and characterized a novel bacterium, designated NBU2967<sup>T</sup> (=KCTC 82912<sup>T</sup>=MCCC 1K06391<sup>T</sup>), for which we propose the name *Meishania litoralis* gen. nov., sp. nov. This strain is classified as a new genus within the family *Flavobacteriaceae*. The strain's ability to process both carbon and sulfur compounds underscores its ecological significance in marine ecosystems. These findings provide novel insights into the ecological functions of the family *Flavobacteriaceae* in coastal tidal flats environments and enhance our understanding of microbial-mediated degradation and transformation of chemical compounds in dynamic coastal ecosystems.

**Keywords** *Flavobacteriaceae*, Coastal tidal flats, Phylogenetic analysis, Comparative genomics

\*Correspondence:

Weiyan Zhang  
zhangweiyan13@126.com  
Lijian Ding  
dinglijian@nbu.edu.cn

Full list of author information is available at the end of the article



© The Author(s) 2025. **Open Access** This article is licensed under a Creative Commons Attribution-NonCommercial-NoDerivatives 4.0 International License, which permits any non-commercial use, sharing, distribution and reproduction in any medium or format, as long as you give appropriate credit to the original author(s) and the source, provide a link to the Creative Commons licence, and indicate if you modified the licensed material. You do not have permission under this licence to share adapted material derived from this article or parts of it. The images or other third party material in this article are included in the article's Creative Commons licence, unless indicated otherwise in a credit line to the material. If material is not included in the article's Creative Commons licence and your intended use is not permitted by statutory regulation or exceeds the permitted use, you will need to obtain permission directly from the copyright holder. To view a copy of this licence, visit <http://creativecommons.org/licenses/by-nc-nd/4.0/>.

## Background

Tidal flats are integral components of marine ecosystems, playing a crucial role in global biogeochemical cycles [1]. Due to their high organic carbon content, tidal flats sustain diverse microbial communities that mediate essential processes in carbon cycling, including organic matter degradation, transformation, and mineralization [2–5]. Advancements in high-throughput sequencing technologies have significantly improved our understanding of microbial diversity, community composition, and functional potential in tidal flats [6–8]. However, many microbial taxa in tidal flats remain poorly characterized, particularly with respect to their metabolic pathways and ecological interactions.

Among the microbial groups frequently found in marine habitats, the family *Flavobacteriaceae* has garnered increasing attention due to its ecological versatility and metabolic adaptability. The family *Flavobacteriaceae* was first established in 1992 [9] and has since undergone three major emendations [10–12]. To date, it includes 188 validly published genera, as documented in the List of Prokaryotic Names with Standing in Nomenclature [13]. *Flavobacteriaceae* are key heterotrophic bacteria in marine ecosystems, playing a crucial role in the degradation of complex organic matter through the secretion of extracellular enzymes [14]. Members of the *Flavobacteriaceae* family are characterized by the presence of a diverse array of carbohydrate-active enzymes (CAZymes), which are encoded within polysaccharide utilization loci (PULs) [5]. These enzymatic systems enable *Flavobacteriaceae* bacteria to efficiently degrade complex polysaccharides derived from marine algae and plants, such as chitin,  $\beta$ -glucans, and cellulose [2, 3, 5].

The degradation products released during this process are subsequently available for utilization by other microorganisms, thereby contributing to the mineralization of organic carbon [3]. Recent studies have highlighted the highly specialized role of *Flavobacteriaceae* in organic carbon degradation, particularly in the regulation of genes encoding glycoside hydrolases, peptidases, and transporters [4, 15]. This specialization renders them promising candidates for industrial applications, particularly in the fields of biodegradation and environmental conservation [5]. Furthermore, the family *Flavobacteriaceae* produce a variety of secondary metabolites that modulate microbial interactions and influence nutrient cycling, especially in carbon-rich marine environments [16, 17].

While the members of the family *Flavobacteriaceae* have been extensively studied in various marine systems, our understanding of their ecological functions in tidal flat environments remains limited. Given the abundance of organic carbon and the unique environmental pressures in tidal flats, it is critical to investigate how members of the family *Flavobacteriaceae* adapt to and function within these habitats. This study investigates a novel *Flavobacteriaceae* strain isolated from the tidal flats of Meishan Island in the East China Sea. Through polyphasic taxonomic analysis, including phylogenetic, physiological, and genomic approaches, the strain's metabolic potential, particularly in organic carbon degradation, was explored. Comparative genomic and pangenome analyses, along with environmental distribution data, highlight the strain's ecological significance and its contribution to carbon cycling in tidal flats ecosystems.

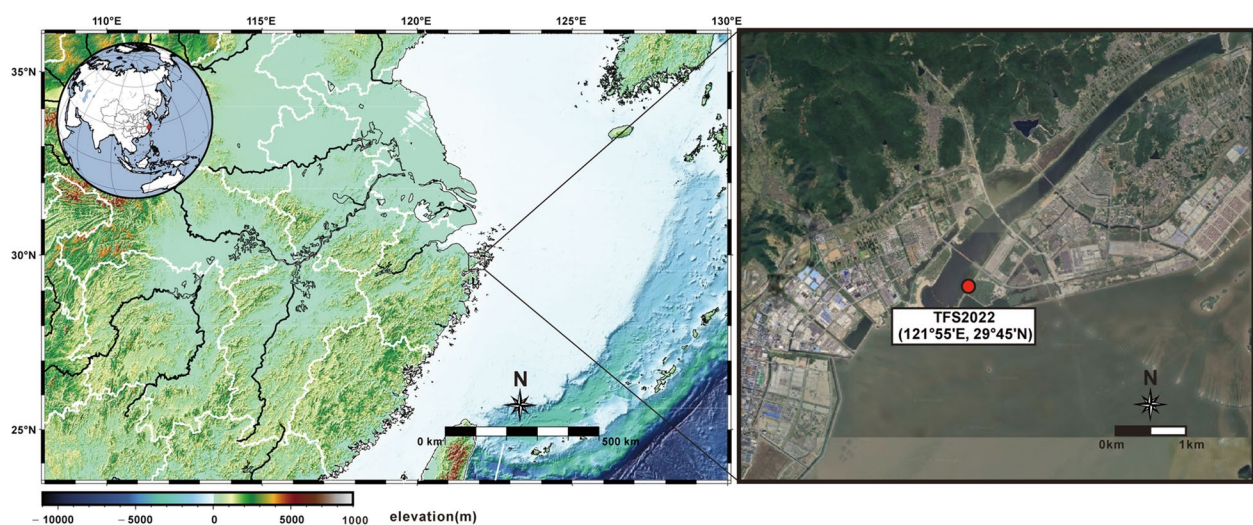


**Fig. 1** Geographic location of Meishan Island and sampling sites. TFS2022, the tidal flats samples collected in 2022

## Methods

### Sample collection and strain isolation

Meishan Island in the East China Sea (121°55'E, 29°45'N) is an open oceanic plain island, with topography sloping from northeast to southwest (Fig. 1). Tidal flats samples were collected in the southwestern part of Meishan Island. The samples were preserved at 4°C before laboratory experiments. For microbial isolation, tidal flat samples were diluted with 2.0% sterilized sea salt solution to a concentration of  $10^{-5}$ . The diluted samples were plated onto Petri dishes containing 1:10 diluted marine agar 2216 (MA; Qingdao Hope Bio-Technology Co., Ltd., China) supplemented with 2.0% (w/v) artificial sea salt, which is composed of sodium chloride (60.67%), magnesium chloride hexahydrate (26.69%), sodium sulfate (9.71%), and calcium chloride (2.93%).

In order to isolate strains with different optimal growth temperatures, inoculated plates were incubated at 24°C, 32°C, and 37°C. After approximately 3 days, colonies began to appear and were subsequently isolated from the respective plates and purified by repeated streaking. All isolated strains were then cultured in marine broth 2216 (MB; Qingdao Hope Bio-Technology Co., Ltd., China) at their respective isolation temperatures and preserved at −80°C in MB supplemented with 25.0% (v/v) glycerol.

### Morphological, physiological, and chemotaxonomic characterization

Cell morphology was analyzed using an optical microscope (BX40, Olympus) and transmission electron microscopy (JEM-1230, JEOL). Cells in the exponential growth phase were cultured on MA plates and subsequently harvested. They were stained with uranyl acetate, fixed onto copper grids, and observed using a transmission electron microscope. Gram staining was conducted following the protocol outlined by Tripathi et al. [18]. Motility was evaluated via direct microscopic observation and by inoculation on semi-solid MA medium containing 0.5% (w/v) agar.

Strain NBU2979<sup>T</sup> was grown in MB at temperatures of 4.0, 10.0, 15.0, 20.0, 25.0, 28.0, 30.0, 35.0, 37.0, 40.0, 45.0, 50.0, and 55.0°C to determine its temperature range. The pH tolerance was evaluated using 30.0 mM buffer systems spanning pH 4.0 to 10.0, adjusted at 0.5-unit intervals: ammonium acetate (pH 4.0–5.0), MES (pH 5.5–6.0), PIPES (pH 6.5–7.0), Tricine (pH 7.5–8.5), and CAPSO (pH 9.0–10.0). NaCl requirement and tolerance range were determined by inoculating into NaCl-free MB basal medium by adding various NaCl concentrations (0, 0.5; 1.0–10.0%, at 1.0% intervals, w/v). All experiments were conducted in quadruplicate, with optical density

at 600 nm ( $OD_{600}$ ) measured after 72 h of incubation at 37.0°C under shaking conditions (140 rpm).

Strain NBU2967<sup>T</sup> was cultured on MB medium at a constant temperature of 37.0°C for physiological characterization. Catalase activity was determined by observing bubble production in a 3.0% (v/v)  $H_2O_2$  solution, while oxidase activity was assessed using the oxidation of 1.0% p-aminodimethylaniline oxalate. Methyl red, Voges-Proskauer tests,  $H_2S$  production, the hydrolysis of starch, casein, Tweens 20, 40, 60, and 80 were conducted following the methods described by Xu et al. [19]. Biochemical and enzymatic activities were evaluated using API ZYM, API 20 NE and API 50 CH strips (bioMérieux) according to the manufacturer's instructions, except for using modified MB in which yeast extract and peptone were replaced by 0.1 g/L yeast extract and 0.01 g/L phenol red. For cell suspension preparation, a 2.0% (w/v) NaCl solution was used instead of the recommended medium. Anaerobic growth was tested using an AnaeroPack-MicroAero (2.5 L; MGC, Japan) system, supplemented with sodium sulfite (5.0 mM), sodium sulfate (20.0 mM), sodium nitrite (5.0 mM), and sodium nitrate (20.0 mM) as electron acceptors. The same media under aerobic conditions were used as controls. Antibiotic susceptibility of strain NBU2967<sup>T</sup> was assessed on MA using antibiotic discs. Susceptibility was determined based on an inhibition zone diameter exceeding 1.5 cm, as described by Zhang et al. [20].

Biomass for chemotaxonomic studies was obtained by cultivating the strain in MB medium at 37.0°C for 72 h under shaking conditions at 140 rpm. Fatty acid methyl ester (FAME) analysis was performed using late exponential-phase cells harvested from MB. The identification and quantification of FAMES were conducted using the Sherlock Microbial Identification System (MIDI) equipped with the standard MIS Library Generation Software (version 6.1), following the manufacturer's protocol. Respiratory quinones were extracted using a chloroform/methanol (2:1, v/v) mixture and analyzed via high-performance liquid chromatography coupled with mass spectrometry (HPLC–MS), employing an Agilent 1200 system and a Thermo Finnigan LCQ DECA XP MAX mass spectrometer [21]. Polar lipids were extracted and separated using two-dimensional thin-layer chromatography (TLC) on silica gel 60  $F_{254}$  plates (Merck). Lipid components were further analyzed according to the method described by Minnikin et al. [22]. Visualization of the TLC plates was achieved by spraying specific reagents: phosphomolybdic acid (5.0% in ethanol) for total lipids,  $\alpha$ -naphthol/sulfuric acid for glycolipids, molybdenum blue for phospholipids, and ninhydrin for amino lipids [23].



### Phylogenetic analysis based on 16S rRNA gene sequences

A total of 61 bacterial strains were isolated from tidal flats samples collected from Meishan Island. The 16S rRNA gene of each strain was amplified using the universal primers 27 F (5'-AGAGTTTGATCCTGGCTCAG-3') and 1492R (5'-GGTTACCTTGTTACGACTT-3') [24], and sequenced by Suzhou Jinwei Zhi Biotechnology Co., Ltd. (Suzhou, China). The resulting sequences were submitted to GenBank under accession numbers PV660043-PV660103. For strain NBU2967<sup>T</sup>, the 16S rRNA gene was further verified and sequenced by cloning into the pMD19-T vector (TaKaRa) and transforming into *Escherichia coli* DH5α, to ensure sequence completeness and accuracy. The full-length 16S rRNA gene sequence (1,490 nt) was compared with closely related species using EzBioCloud's Identify Service (<http://www.ezbiocloud.net/identify>) [25] and the BLAST database (<https://blast.ncbi.nlm.nih.gov/Blast.cgi>). Phylogenetic trees were reconstructed using IQ-TREE v1.6.1 software [26] via three different methods: neighbor-joining [27], maximum-parsimony [28], and maximum-likelihood [29]. Evolutionary distances for the neighbor-joining method were computed using the Kimura 2-parameter model [30], and bootstrap analyses with 1,000 replications assessed tree robustness. A single neighbor-joining phylogenetic tree was also constructed based on the aligned 16S rRNA gene sequences of the 61 isolated strains to investigate their evolutionary relationships.

For phylogenetic analysis, 16S rRNA sequence data were used to identify the six closest related genera within the family *Flavobacteriaceae*, represented by the following strains: *Maribacter algicola* PoM-212<sup>T</sup> [31], *M. sedimenticola* KMM 3903<sup>T</sup> [32], *Aggregatimonas sangjinii* F202Z8<sup>T</sup> [33], *Costertonia aggregata* KCCM42265<sup>T</sup> [34], *Ulvibacterium marinum* CCMM003<sup>T</sup> [35], *Pseudozobellia thermophila* DSM 19858<sup>T</sup> [36], and *Pareuzobryella sediminis* S2-4-21<sup>T</sup> [37]. Among the genus *Maribacter*, both the type strain (*M. sedimenticola* KMM 3903<sup>T</sup>) and the species showing the highest 16S rRNA gene sequence similarity to strain NBU2967<sup>T</sup> (*M. algicola* PoM-212<sup>T</sup>) were included. These strains were selected for comparative characterization alongside strain NBU2967<sup>T</sup>.

### Genome sequencing, assembly, and analysis

The whole genome of strain NBU2967<sup>T</sup> was sequenced using the Illumina HiSeq 4000 platform (Illumina) at the Beijing Genomics Institute (Shenzhen, China) [20]. Paired-end fragment libraries were prepared and sequenced according to the standard Illumina HiSeq 4000 protocol. Low-quality reads (those with consecutive bases covered by fewer than five reads) were filtered out, and the high-quality reads were assembled using SOAPdenovo v1.05 software [38]. The genomic DNA G +

C content was calculated from the assembled genome sequence.

Annotation of the genomic features of strain NBU2967<sup>T</sup> was performed using Prokka v1.14.6, a rapid and comprehensive genome annotation tool [39]. Prokka integrates several software packages, including Prodigal [40] for coding sequence (CDS) prediction, RNAmmer [41] for ribosomal RNA gene identification, Aragorn [42] for tRNA gene detection, SignalP [43] for signal peptide prediction, and Infernal [44] for non-coding RNA identification. Prokka generates output files in standard formats, including FAA, GFF, and GBK, which were used for downstream analyses. To supplement these results, Rapid Annotation using Subsystem Technology (RAST) was employed for the functional annotation of open reading frames (ORFs) [45]. The combination of Prokka and RAST ensured comprehensive and accurate genome annotation. For metabolic pathway analysis, metabolic pathways were reconstructed using KEGG's BlastKOALA annotation service [46].

Genomic data for reference strains within the family *Flavobacteriaceae*, selected based on their high 16S rRNA sequence similarity to strain NBU2967<sup>T</sup>, were retrieved from the NCBI Genome Database. These strains included *M. algicola* PoM-212<sup>T</sup>, *M. cobaltidurans* B1<sup>T</sup> [47], *M. aurantiacus* CDA4<sup>T</sup> [48], *M. flavus* KCTC 42508<sup>T</sup> [49], *M. arenosus* CAU 1321<sup>T</sup> [50], *M. litopenaei* HL-LV01<sup>T</sup> [51], *M. thermophilus* HT7-2<sup>T</sup> [52], *Pricia antarctica* DSM 23421<sup>T</sup> [53], *Pelagihabitans pacificus* TP-CH-4<sup>T</sup> [54], *M. luteus* RZ05<sup>T</sup> [55], *M. aquimaris* ANRC-HE7<sup>T</sup> [56], *M. polysiphoniae* DSM 23514<sup>T</sup> [57], *A. sangjinii* F202Z8<sup>T</sup>, *C. aggregata* KCCM42265<sup>T</sup>, *U. marinum* CCMM003<sup>T</sup>, *Ps. thermophila* DSM 19858<sup>T</sup>, and *Pa. sediminis* S2-4-21<sup>T</sup>. The average nucleotide identity (ANI) values between strain NBU2967<sup>T</sup> and reference strains within the family *Flavobacteriaceae* were calculated using the ANI calculator (<http://enve-omics.ce.gatech.edu/ani/>) [58]. The average amino acid identity (AAI) was estimated using the EzAAI Calculator online service (<http://leb.snu.ac.kr/ezaai>) [59]. Digital DNA-DNA hybridization (dDDH) values were computed via the genome-to-genome distance calculator (GGDC) server version 2.1 [60]. To explore the phylogenomic relationships between strain NBU2967<sup>T</sup> and related taxa, a genome-based phylogenomic tree was constructed using the Type Strain Genome Server (TYGS) [61]. The combined use of ANI, AAI, dDDH, and phylogenomic tree reconstruction ensured robust species delineation and supported the taxonomic classification of strain NBU2967<sup>T</sup> [62].

The CAZymes profiles and gene clusters of strain NBU2967<sup>T</sup> and reference strains within the family *Flavobacteriaceae* were analyzed using the dbCAN3 server

(<https://bcbl.unl.edu/dbCAN2/blast.php>) [63]. Protein sequences predicted by Prokka were submitted to the dbCAN3 server, and annotation was performed using HMMER (E-value < 1e-15) with the CAZymes domain HMM database [64]. Biosynthetic gene clusters (BGCs) across all genomes were identified using antiSMASH v5.0 [65]. The GBK files generated by Prokka served as input data for this analysis.

### Protein structure prediction

Protein structures related to metabolism were predicted using the Phyre2.2 web server in intensive mode [66]. The predicted structures were then compared to known protein structures by querying structural databases using Foldseek (<https://search.foldseek.com/>) [67]. Structural alignments between the predicted and target proteins were performed with the US-align tool (<https://zhanggroup.org/US-align/>) [68], and visualizations of protein structures were generated using PyMOL software.

### Pangenome analysis

The pangenome, encompassing all gene clusters in a group, is divided into the core and accessory genomes [69]. The core genome includes conserved functional genes found across all strains, while the accessory genome consists of dispensable genes found in some strains and strain-specific genes (singletons) unique to a single strain [70]. The resulting GFF files predicted by Prokka were analyzed using Roary with the default settings to determine the pangenome structure [71]. The IPGA v1.09 (Integrated Prokaryotes Genome and Pangenome Analysis service; <https://nmcdc.cn/ipga/>) was used to plot the Tettelin best-fit curve, which describes the changes in pangenome and core genome sizes and their regression trends [72].

### Environmental distribution

The distribution and habitat preferences of the newly described genus *Meishania* globally were assessed using the analytical tools from the Microbe Atlas Project (MAP). The study was conducted with a rigorous 96% sequence similarity threshold. Microbial community abundance was assessed through MAPseq, a closed reference method for analyzing ribosomal RNA sequences [73].

## Results and discussion

### Morphological, physiological, and chemotaxonomic characteristics

Morphological analysis of strain NBU2967<sup>T</sup> revealed that the cells are Gram-negative, rod-shaped, non-flagellated, and measure approximately 0.6–0.8 × 1.2–1.6 μm (Fig.

S1). After 72 h of incubation on MA medium at 37.0°C, colonies were approximately 1 mm in diameter, circular, raised, and exhibited an orange-yellow color. Growth was observed within a pH range of 5.5–8.5, with an optimum at pH 6.5 (Fig. S2A); a temperature range of 10.0–40.0°C, with an optimum at 37.0°C; and NaCl concentrations of 1.0–5.0% (w/v), with an optimum at 2.0%. A pronounced exponential phase was observed between 24 and 36 h of incubation under optimal growth conditions (Fig. S2B). No growth occurred under anaerobic conditions, even after two weeks of incubation on modified MA medium supplemented with various electron acceptors, indicating that strain NBU2967<sup>T</sup> is strictly aerobic.

Biochemical tests indicated that strain NBU2967<sup>T</sup> was positive for catalase and oxidase activities, the methyl red test, hydrolysis of Tweens 20, 40, 60, and 80. Negative results were obtained for H<sub>2</sub>S production, Voges-Proskauer test, hydrolysis of starch and casein. Enzymatic activity profiling using the API ZYM test kit revealed positive reactions for alkaline phosphatase, esterase (C4), lipase (C8 and C14), leucine arylamidase, valine arylamidase, acid phosphatase, naphthol-AS-BI-phosphohydrolase, α-galactosidase, β-galactosidase, α-glucosidase, β-glucosidase, N-acetyl-glucosaminidase, α-mannosidase, and β-fucosidase. The API 20 NE test kit showed positive activity for aesculin hydrolysis and β-galactosidase, while the API 50 CH test kit demonstrated positive utilization of a wide range of carbohydrates and glycosides, including D-arabinose, L-arabinose, D-ribose, D-xylose, L-xylose, β-methyl-D-xylopyranoside, D-galactose, D-glucose, D-fructose, D-mannose, α-methyl-D-mannopyranoside, α-methyl-D-glucopyranoside, N-acetyl-β-D-glucosamine, amygdalin, arbutin, aesculin, salicin, cellobiose, maltose, lactose, melibiose, sucrose, trehalose, melezitose, raffinose, gentiobiose, D-turanose, D-lyxose, D-tagatose, D-fucose, L-fucose, and 2-ketoglucuronate. Antibiotic susceptibility testing revealed sensitivity to a broad spectrum of antibiotics, including lincomycin, clindamycin, tetracycline, doxycycline, erythromycin, ofloxacin, vancomycin, chloramphenicol, cephalexin, cefoxitin, amoxicillin, rifampicin, cephalothin, carbenicillin, ciprofloxacin, and ampicillin.

The major fatty acids (≥ 10%) were identified as iso-C<sub>15:0</sub>, iso-C<sub>17:0</sub> 3-OH, and Summed Feature 1 (iso-C<sub>15:1</sub> H/C<sub>13:0</sub> 3-OH). A detailed composition of all fatty acids present at levels greater than 1% is provided in Table S1. The sole respiratory quinone was menaquinone-6. The polar lipid profile included phosphatidylethanolamine (PE), aminophospholipid (APL), two unidentified lipids (Ls), two unidentified phospholipids (PLs), and three unidentified aminolipids (Als) (Fig. S3). Key characteristics distinguishing strain NBU2967<sup>T</sup> from closely related genera

**Table 1** Characteristics differentiating strain NBU2967<sup>T</sup> from its reference strains within the family *Flavobacteriaceae*. The reference strains represent the six closest related genera

Characteristic	1	2	3	4	5	6	7	8
Colony color	Orange-yellow	Orange	Yellow	Orange	Orange	Yellow	Orange	Light-orange
Motility	non-motile	non-motile	non-motile	motile	motile	non-motile	motile	non-motile
Cell size (μm)	0.6–0.8 × 1.2–1.6	0.3–0.4 × 2.7–3.3	0.5–0.7 × 2.0–10.0	0.3–0.5 × 0.9–2.7	0.3–0.4–0.5– 0.6	0.5–0.6 × 1.7–2.3	0.2–0.4 × 1.2–3.0	0.5–0.7 × 1.6–1.7
Temperature range (optimum, °C)	10–40 (37)	20–40 (30)	4–33(22–24)	15–33 (30)	10–35 (29)	8–42 (30)	4–49 (28)	15–40 (30–35)
pH range (optimum)	5.5–8.5 (6.5)	5.0–8.5 (5.0–5.5)	5.5–10.0(7.5–8.5)	6.5–7.5 (7.0)	6.5–9.0 (7.5)	6.0–9.0 (7.0)	ND	6.0–9.0 (ND)
NaCl range (optimum) (% w/v)	1.0–5.0 (2.0)	0.5–5.0 (2.0–3.0)	1.0–6.0(1.5–2.0)	2.5–4.5 (4.0)	1.5–12.0 (3.0)	2.0–5.0 (4.0)	0.5–8.0 (4.0–5.0)	0.5–10.0 (2.0)
Oxidase/catalase activity	+/+	+/+	+/+	+/+	+/+	-/-	+/+	-/+
Polar lipids	PE, APL, L, PL, AL	PE, AL, L	ND	PE, AL, L	ND	PE, L	ND	PE, AL, L
Main fatty acids (> 10%)	iso-C <sub>15:0</sub> , iso-C <sub>17:0</sub> 3-OH, and summed Feature 1*	iso-C <sub>15:1</sub> , iso-C <sub>15:0</sub> , iso-C <sub>17:0</sub> 3-OH, and summed feature 3*	iso-C <sub>15:0</sub> , iso-C <sub>15:1</sub> , C <sub>15:0</sub> , and iso-C <sub>17:0</sub> 3-OH	iso-C <sub>15:0</sub> , iso-C <sub>15:1</sub> G, iso-C <sub>17:0</sub> 3-OH, and summed feature 3*	iso-C <sub>15:0</sub> , iso-C <sub>15:1</sub> ω10, C <sub>15:0</sub> , and C <sub>16:1</sub> ω9	iso-C <sub>15:0</sub> , iso-C <sub>15:1</sub> G, iso-C <sub>17:0</sub> 3-OH, and summed feature 3*	iso-C <sub>15:0</sub> , iso-C <sub>17:0</sub> 3-OH, and iso-C <sub>15:1</sub> G	iso-C <sub>15:0</sub> , iso-C <sub>17:0</sub> 3-OH, iso-C <sub>15:1</sub> G

Taxa: 1, strain NBU2967<sup>T</sup>; 2, *M. algicola* PoM-212<sup>T</sup>; 3, *M. sedimenticola* KMM 3903<sup>T</sup>; 4, *A. sangjinii* F202Z8<sup>T</sup>; 5, *C. aggregata* KCCM42265<sup>T</sup>; 6, *U. marinum* CCMM003<sup>T</sup>; 7, *Ps. thermophila* DSM 19858<sup>T</sup>; 8, *Pa. sediminis* S2-4–21<sup>T</sup>. Data for strains 2, 3, 4, 5, 6, 7, and 8 are from Khan et al. [31], Nedashkovskaya et al. [32], Chung et al. [33], Kwon et al. [34], Zhang et al. [35], Nedashkovskaya et al. [36], and Huang et al. [37], respectively. PE, phosphatidylethanolamine; APL, aminophospholipid; PL, phospholipid; AL, amidolipid; L, lipid. -, negative. +, positive. ND, no data

\* Summed features are groups of two or three fatty acids that cannot be separated by GLC using the MIDI system. Summed Feature 1 consisted iso-C<sub>15:1</sub> H and/or C<sub>13:0</sub> 3OH and summed feature 3 consisted C<sub>16:1</sub> ω7c and/or C<sub>16:1</sub> ω6c

within the family *Flavobacteriaceae* are summarized in Table 1.

### Phylogenetic analysis based on the 16S rRNA gene sequences

The complete 16S rRNA gene sequence of strain NBU2967<sup>T</sup> (1,490 nt; GenBank accession number: MZ025914) was successfully obtained through PCR amplification and sequencing. A comparative analysis of this sequence using the EzBioCloud and NCBI GenBank databases revealed that strain NBU2967<sup>T</sup> exhibited the highest sequence similarity to *M. algicola* PoM-212<sup>T</sup> (94.88%), followed by *M. cobaltidurans* B1<sup>T</sup> (94.82%), *M. aurantiacus* CDA4<sup>T</sup> (94.33%), *M. halichondriae* Hal144<sup>T</sup> (94.27%), *M. flavus* KCTC 42508<sup>T</sup> (94.20%), and *M. arenosus* CAU 1321<sup>T</sup> (94.20%). Similarity to all other strains was less than 94.20%.

Phylogenetic trees constructed using the neighbor-joining, maximum-likelihood, and maximum-parsimony methods consistently demonstrated that strain NBU2967<sup>T</sup> formed a distinct lineage within the family *Flavobacteriaceae* (Fig. 2, Figs. S4, S5). Importantly, the 16S rRNA gene sequence similarities between strain NBU2967<sup>T</sup> and its closest phylogenetic neighbors were

below the established thresholds for bacterial genus (< 95.0%) delineation [74, 75]. These results suggest that strain NBU2967<sup>T</sup> potentially represents a novel genus within the family *Flavobacteriaceae*.

A total of 61 bacterial strains were isolated. Based on 16S rRNA gene sequence comparisons with validly published species, these isolates were assigned to 50 species belonging to 6 phyla, 9 classes, 16 orders, 26 families, and 33 genera. To investigate the evolutionary relationships among the isolates, a neighbor-joining phylogenetic tree was constructed based on aligned 16S rRNA gene sequences from all 61 strains (Fig. S6). The neighbor-joining tree revealed that these strains were distributed across multiple phylogenetically distinct lineages, forming several well-supported clades. Despite being recovered from the same sampling site, the strains exhibited considerable phylogenetic diversity, indicating a taxonomically complex microbial community. This phylogenetic topology reflects a heterogeneous and evolutionarily diverse bacterial population in the coastal tidal flat habitat.

### Genomic characteristics

The draft genome of strain NBU2967<sup>T</sup> has a total length of 3,819,109 bp and is composed of 18 contigs, with a

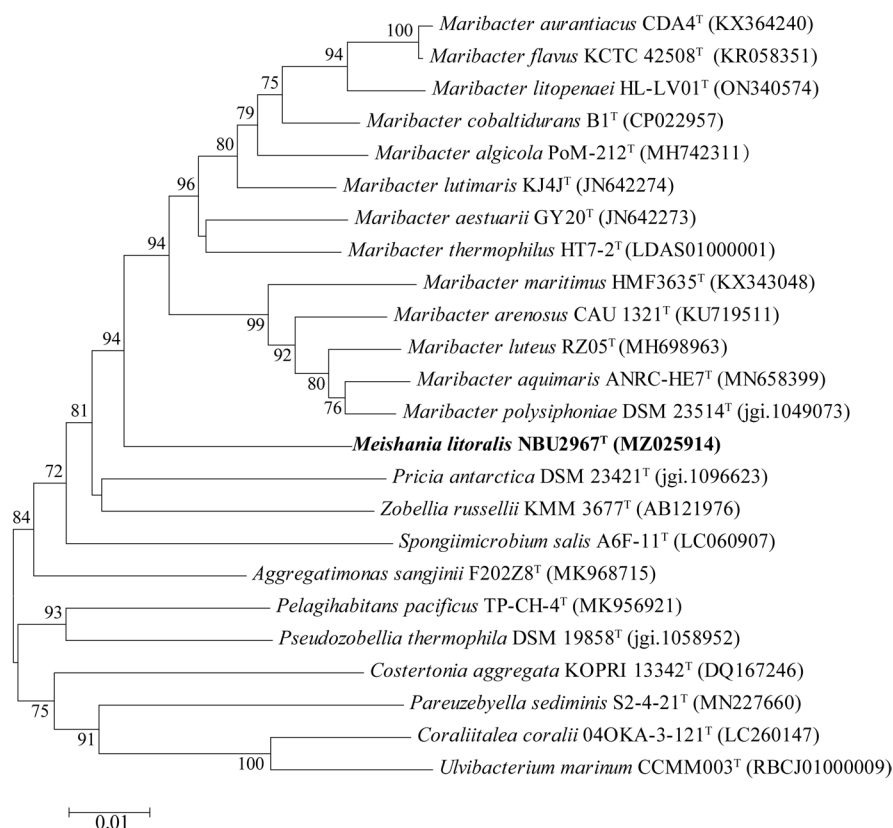


**Fig. 2** Neighbor-joining phylogenetic tree based on 16S rRNA gene sequences. Bootstrap values are shown at nodes as percentages of 1000 replicates. Values under 70% are hidden. Bar, 0.01 changes per nucleotide position

genomic DNA G + C content of 42.5% (Fig. S7 A). The draft genome comprises 3,412 genes, including 3,364 protein-coding genes, 14 pseudogenes, and 44 RNA genes (3 rRNA genes, 37 tRNA genes, and 4 non-coding RNA genes). A comparison of the genomic features of strain NBU2967<sup>T</sup> with 16 reference strains within the family *Flavobacteriaceae* is provided in Table S2. Genome annotation using the RAST subsystem categorization revealed that the identified genes are distributed across 22 functional categories, as illustrated in Fig. S7B.

RAST predictions showed that the genome of strain NBU2967<sup>T</sup> is involved in several important metabolic and biological processes. The most prominent categories were protein families: genetic information processing (173 genes) and genetic information processing (155 genes), suggesting that the strain plays a significant role in genetic information transfer and regulation. Additionally, carbohydrate metabolism (156 genes) indicates the strain's strong ability to metabolize carbon, allowing it to efficiently utilize carbon sources. The most prominent categories were protein families involved in genetic information processing (173 genes) and cellular functions related to genetic information (155 genes), suggesting

that the strain has a strong capacity for genetic regulation and information processing.

#### Overall genomic relatedness and phylogenomics

The ANI, AAI, and dDDH values were calculated to identify the genomic similarities of strain NBU2967<sup>T</sup> with reference strains within the family *Flavobacteriaceae* (Fig. 3). The ANI values between strain NBU2967<sup>T</sup> and reference strains within the family *Flavobacteriaceae* ranged from 70.5% to 71.6%, which is below the genus-level threshold of 73.98% (95% confidence interval: 73.34–74.62%) [76]. Similarly, the AAI values ranged from 72.4% to 77.5%, consistent with the genus differentiation range of 60–80% within the family *Flavobacteriaceae* [77, 78]. The dDDH values were calculated to be between 16.8% and 19.6%, significantly lower than the proposed 70% threshold for species delineation [79]. Phylogenomic analysis based on whole-genome sequences further supports the distinct evolutionary position of strain NBU2967<sup>T</sup>, as it forms a separate lineage within the family *Flavobacteriaceae* (Fig. S8).

Collectively, these findings strongly indicate that strain NBU2967<sup>T</sup> represents a novel taxon with unique genomic



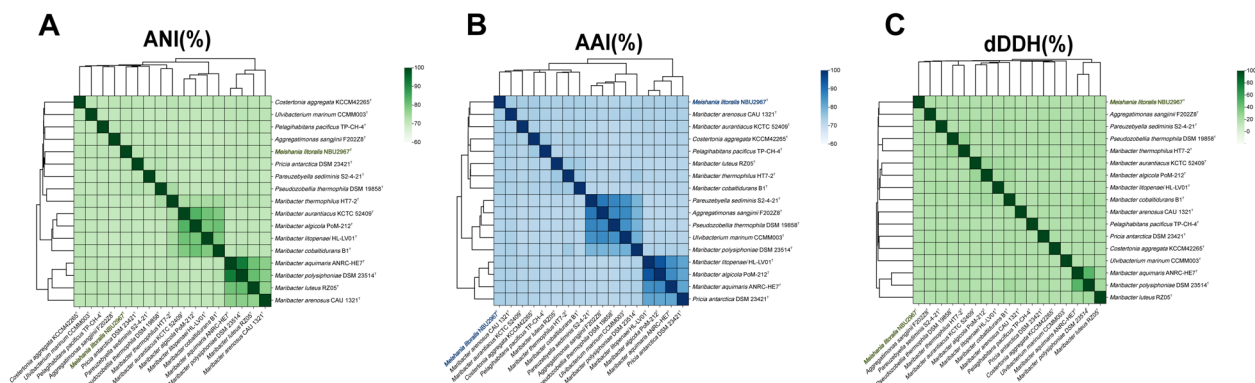


**Fig. 3** Genomic similarities between strain NBU2967<sup>T</sup> and reference strains within the family *Flavobacteriaceae*. **(A)**, The ANI values between strain NBU2967<sup>T</sup> and reference strains within the family *Flavobacteriaceae*; **(B)**, The AAI values between strain NBU2967<sup>T</sup> and reference strains within the family *Flavobacteriaceae*; **(C)**, The dDDH values between strain NBU2967<sup>T</sup> and reference strains within the family *Flavobacteriaceae*

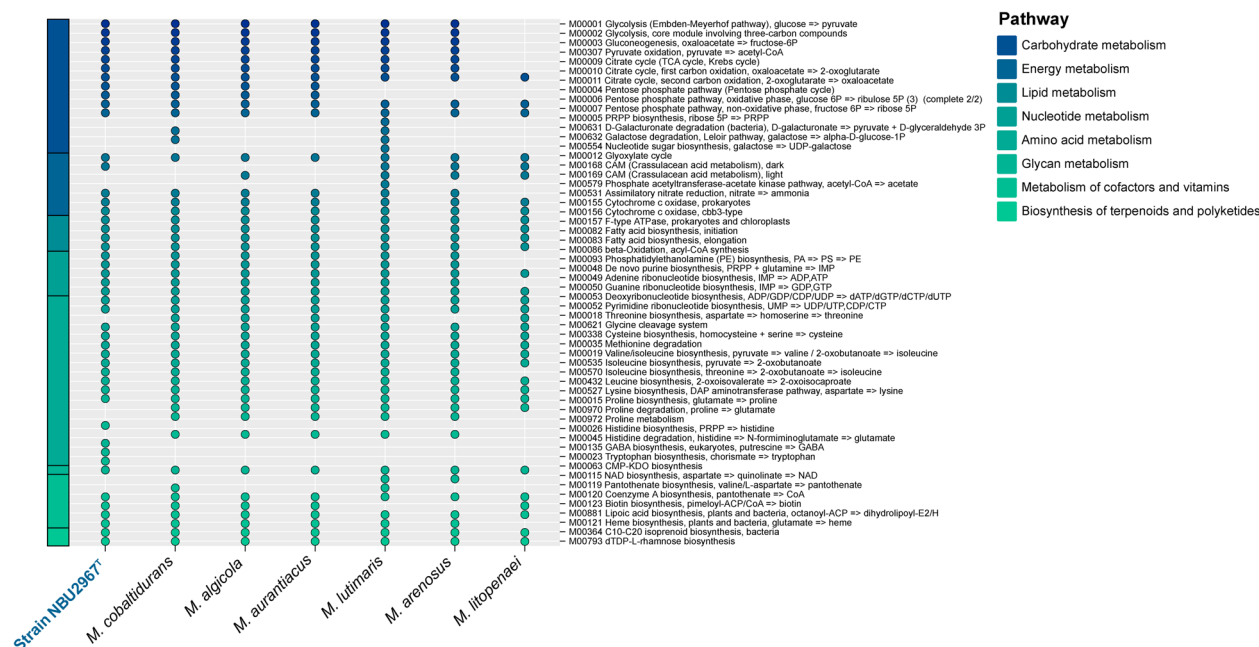


**Fig. 4** The metabolic module integrity of strain NBU2967<sup>T</sup>, along reference strains. The solid circles and hollow circles indicate that the metabolic pathways were complete and incomplete, respectively

and evolutionary characteristics, justifying its classification as a new genus within the family *Flavobacteriaceae*.

### Evaluation of the metabolic and ecological potential

#### Metabolic pathway analysis

The KEGG analysis of strain NBU2967<sup>T</sup> and reference strains within the family *Flavobacteriaceae* revealed a high degree of metabolic adaptability and diversity across this taxonomic group (Fig. 4). These include pathways involved in carbohydrate metabolism and energy production. Complete metabolic pathways, such as glycolysis (M00001), the citric acid cycle (M00009), and the pentose

phosphate pathway (M00004), demonstrate the ability of these strains to efficiently utilize carbon sources (Fig. 5). Genome analysis revealed that strain NBU2967<sup>T</sup> encodes a complete *cbb*<sub>3</sub>-type cytochrome c oxidase complex, along with additional cytochrome c oxidase subunits and heme-copper oxidases. These components constitute a functional terminal oxidase system that supports oxygen respiration [80]. The presence of these genes is consistent with the organism's obligate aerobic phenotype observed in culture. Strain NBU2967<sup>T</sup> also exhibited a unique metabolic pathway not possessed by other strains: Gamma-Aminobutyric Acid (GABA) biosynthesis, eukaryotes,



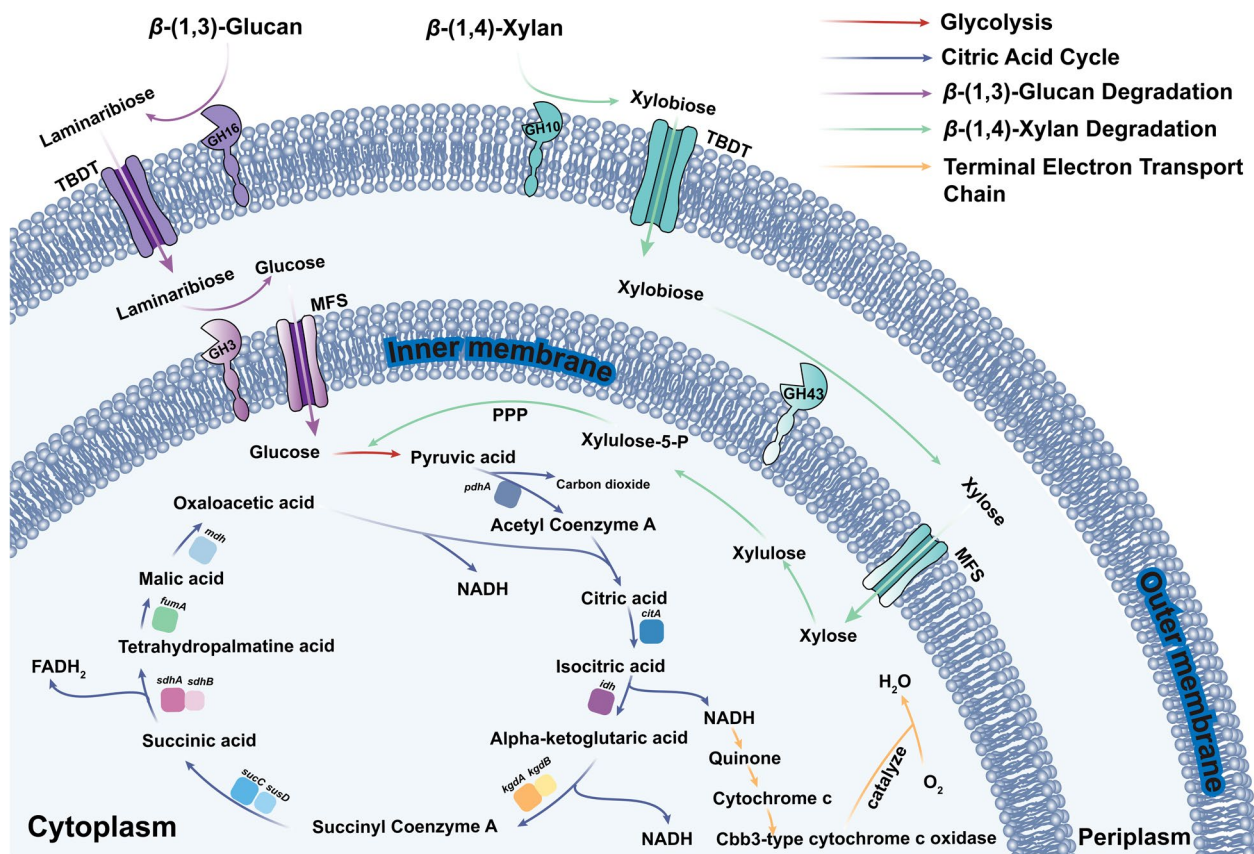


**Fig. 5** Integrated pathways of  $\beta$ -(1,3)-glucan and  $\beta$ -(1,4)-xylan degradation with central carbon metabolism and terminal electron transport in bacteria. NADH/FADH<sub>2</sub>, Reduced cofactors that donate electrons to the respiratory chain; MFS, major facilitator superfamily; TBDT, TonB-dependent transporter; PPP, pentose phosphate pathway

putrescine => GABA(M00135). It has been reported that GABA is widely utilized by microorganisms as an important signaling molecule and osmoprotectant in response to various abiotic stresses (e.g., high salinity, drought, darkness, and cytoplasmic acidification) [81]. Moreover, GABA metabolism is closely associated with the regulation of the cellular carbon/nitrogen balance, energy homeostasis, and redox state modulation [81]. Strain NBU2967<sup>T</sup> possesses the ability to biosynthesize GABA, suggesting that it may have enhanced capabilities for environmental stress response and osmoregulation, which could contribute to its survival and colonization in diverse ecological environments.

In order to further understand its metabolic mechanisms in the marine tidal flat environment, its genome was analyzed and found to encode a variety of key enzymes related to carbon and sulfur metabolism, suggesting that the strain plays an important ecological role in organic matter transformation and nutrient cycling (Fig. 6). The analysis results showed that the strain contained  $\alpha$ -glucuronidase, an enzyme that plays a crucial role in the degradation of plant cell wall polysaccharides,

particularly in the hydrolysis of glucuronic acid-containing xylans [82]. Meanwhile, endo- $\beta$ -(1,3)-glucanase was identified, an enzyme that targets  $\beta$ -(1,3)-glucan, a component of plant cell walls and fungal cell membranes [83]. This enzyme is critical for breaking down complex polysaccharides such as laminarin, a major carbohydrate in marine algae, and mixed-linkage glucans commonly found in cereals [84]. The presence of both  $\alpha$ -glucuronidase and endo- $\beta$ -(1,3)-glucanase suggests that this strain is well-equipped to degrade a broad spectrum of polysaccharides, thereby enhancing its ability to utilize organic matter from diverse sources. The strain also possesses endo-1,4- $\beta$ -xylanase, which is capable of hydrolyzing the  $\beta$ -1,4-glycosidic bond in xylan, further enhancing its ability to degrade plant-derived carbon sources [85]. The combined action of these enzymes endowed the microorganism with strong adaptability and metabolic potential in the carbon-rich environment of marine tidal flats.

In addition to its carbon metabolizing capacity, the strain showed equally remarkable potential in sulfur metabolism. The genome analysis revealed the presence

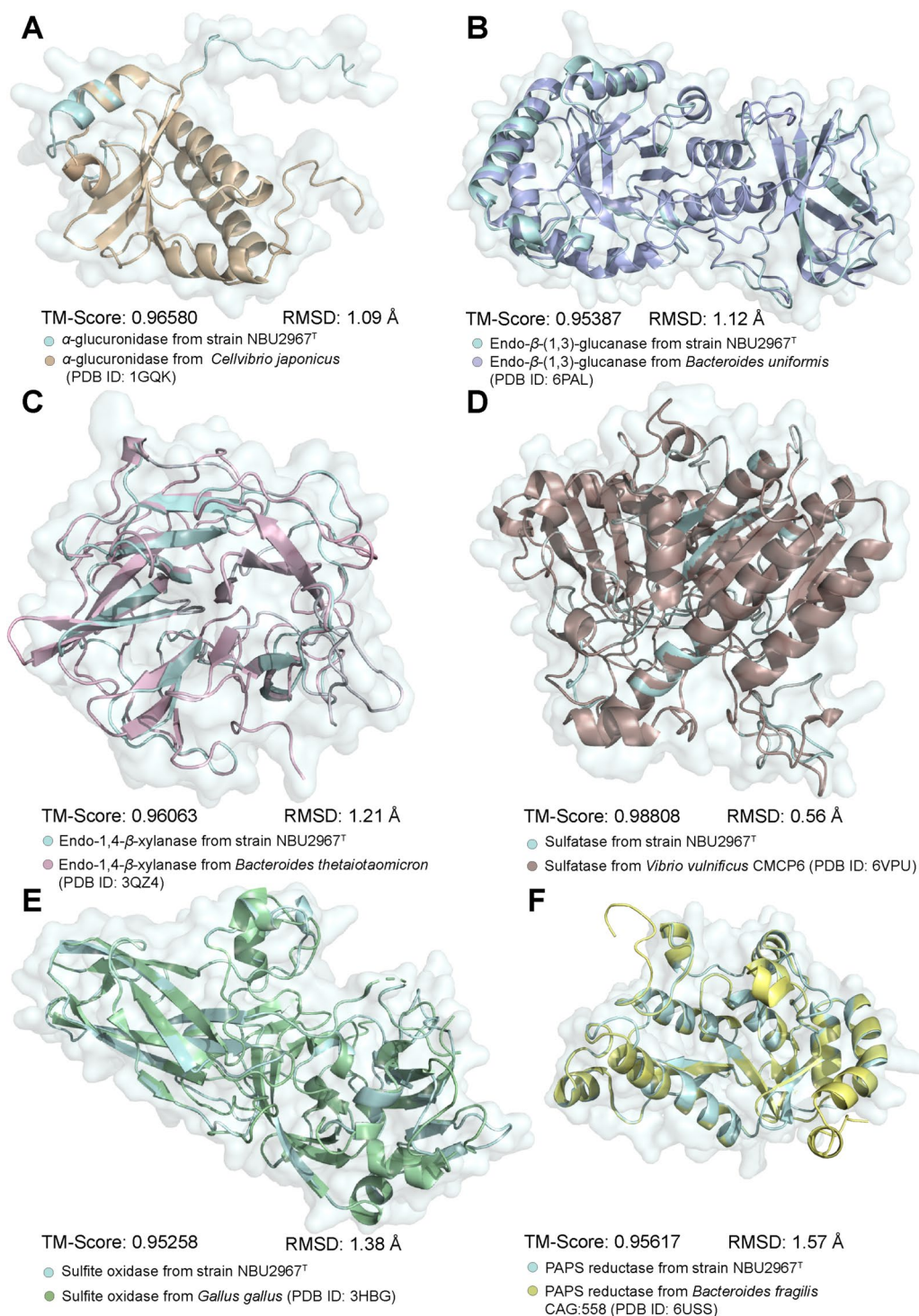


**Fig. 6** Protein Structural Analysis. (A), Structure alignment of the α-glucuronidase from strain NBU2967<sup>T</sup> with that from *Cellvibrio japonicus* (PDB ID: 1GQK); (B), Structure alignment of the endo-β-(1,3)-glucanase from strain NBU2967<sup>T</sup> with that from *Bacteroides uniformis* (PDB ID: 6PAL); (C), Structure alignment of the endo-1,4-β-xylanase from strain NBU2967<sup>T</sup> with that from *Bacteroides thetaiotaomicron* (PDB ID: 3QZ4); (D), Structure alignment of the sulfatase from strain NBU2967<sup>T</sup> with that from *Vibrio vulnificus* (PDB ID: 6VPU); (E), Structure alignment of the sulfite oxidase from strain NBU2967<sup>T</sup> with that from *Gallus gallus* (PDB ID: 3HBG); (F), Structure alignment of the PAPS reductase from strain NBU2967<sup>T</sup> with that from *Bacteroides fragilis* CAG:558 (PDB ID: 6USS). RMSD and TM-Score values are presented

of sulfatase, an enzyme capable of hydrolyzing a wide range of organic sulfate compounds, including sulfated marine polysaccharides, which are common in marine ecosystems [86]. This hydrolysis process releases inorganic sulfate and provides precursors for subsequent sulfur assimilation or reduction processes, thereby contributing to sulfur cycling in marine environments [87]. In addition, sulfite oxidase was identified. Sulfite oxidase plays a critical role in sulfur metabolism by catalyzing the oxidation of sulfite to sulfate, an essential step in the microbial sulfur cycle [88]. The mechanism not only helps detoxify sulfite, which is toxic to cells, but also facilitates sulfur cycling in microbial communities. Phosphoadenosine phosphosulfate (PAPS) reductase was also detected, which plays a key role in reducing PAPS to sulfide, an essential step in the assimilation of sulfate into biologically active sulfur compounds like cysteine [89]. The combined action of these sulfur-metabolizing enzymes allows the strain to significantly contribute to the sulfur cycle, aiding in the transformation and recycling of sulfur within marine tidal flat ecosystems.

Structural alignment of putative proteins from strain NBU2967<sup>T</sup> with verified enzymes revealed high conformity: putative  $\alpha$ -glucuronidase exhibited a root mean square deviation (RMSD) of 1.09 Å compared to a validated  $\alpha$ -glucuronidase (PDB ID: 1GQK); putative endo- $\beta$ -(1,3)-glucanase exhibited a RMSD of 1.12 Å compared to a validated endo- $\beta$ -(1,3)-glucanase (PDB ID: 6PAL); putative endo-1,4- $\beta$ -xylanase exhibited a RMSD of 1.21 Å compared to a validated endo-1,4- $\beta$ -xylanase (PDB ID: 3QZ4); putative sulfatase exhibited a RMSD of 0.56 Å compared to a validated sulfatase (PDB ID: 6VPU); putative sulfite oxidase exhibited a RMSD of 1.38 Å compared to a validated sulfite oxidase (PDB ID: 3HBG); and putative PAPS reductase exhibited a RMSD of 1.57 Å compared to a validated PAPS reductase (PDB ID: 6USS) (Fig. 6). Structural modeling confirmed functional conservation of these enzymes.

#### Analysis of CAZymes predicted by dbCAN3

Strain NBU2967<sup>T</sup> and reference strains within the family *Flavobacteriaceae* harbored extensive reservoirs of CAZymes. Total CAZymes predicted by dbCAN3 across the genomes of these strains ranged from 115 to 277 per strain (Fig. 7). The most abundant CAZyme families in

strain NBU2967<sup>T</sup> were Glycoside Hydrolases (GHs) (60 species), followed by Glycosyltransferases (GTs) (46 species), Carbohydrate Esterases (CEs) (17 species), Carbohydrate Binding Modules (CBMs) (13 species), Auxiliary Activities (AAs) (8 species), and Polysaccharide Lyase (PL) (1 species), respectively.

GH enzymes catalyze the cleavage of glycosidic bonds in a wide range of substrates, from small glucosinolates to complex polysaccharides, and are classified based on their catalytic mechanisms [90]. Among the 82 GH enzymes identified in the genomes of strain NBU2967<sup>T</sup> and reference strains within the family *Flavobacteriaceae*, GH188 enzymes accounted for the highest proportion, ranging from 2.9% to 72.7% (Table S3). GH188 enzymes, a specialized class of glycoside hydrolases, exhibit unique structural and catalytic properties. They are capable of breaking down sulfoquinovosyl diacylglycerols (SQDG) [91], thereby releasing sulfur and carbon sources that can be utilized by bacteria. This activity facilitates the decomposition of organic carbon, supports microbial food webs, and promotes coupled sulfur and carbon metabolism, thereby contributing to carbon cycling in tidal flats environments.

GT enzymes play a fundamental role in life processes by catalyzing the transfer of saccharide moieties from sugar nucleotide donors to acceptor molecules [92]. They are essential for the biosynthesis of oligosaccharides and N- and O-linked glycoconjugates. Among the GT families identified in strain NBU2967<sup>T</sup> and reference strains within the family *Flavobacteriaceae*, GT4 and GT2 accounted for the highest proportions (Table S3). These two families are believed to represent the ancestral sources of GH families [93]. According to the dbCAN-seq database, GT2 and GT4 constitute 30% and 28%, respectively, of the total GT enzymes in marine environments, underscoring their widespread presence among marine organisms [94]. The combined GH and GT gene ratio to total protein-coding genes in strain NBU2967<sup>T</sup> and reference strains within the family *Flavobacteriaceae* ranged from 2.3% to 5.4%, significantly higher than the typical ratio of 1–3% observed in other bacterial taxa [95]. This elevated ratio reflects an enhanced capacity for polysaccharide metabolism, suggesting a specialized adaptation for efficient carbohydrate utilization in marine environments.

(See figure on next page.)

**Fig. 7** Taxonomic annotation and distribution of CAZymes in strain NBU2967<sup>T</sup> and reference strains. The upper chord plot illustrates the number of CAZymes annotated in strain NBU2967<sup>T</sup> and reference strains within the family *Flavobacteriaceae* compared to the records in the dbCAN-seq database. The lower bubble plot illustrates the distribution of CAZymes families in strain NBU2967<sup>T</sup> and reference strains within the family *Flavobacteriaceae*, and types containing more than 8 CAZymes per strain have been labeled in the plot. Detailed information can be found in Table S3



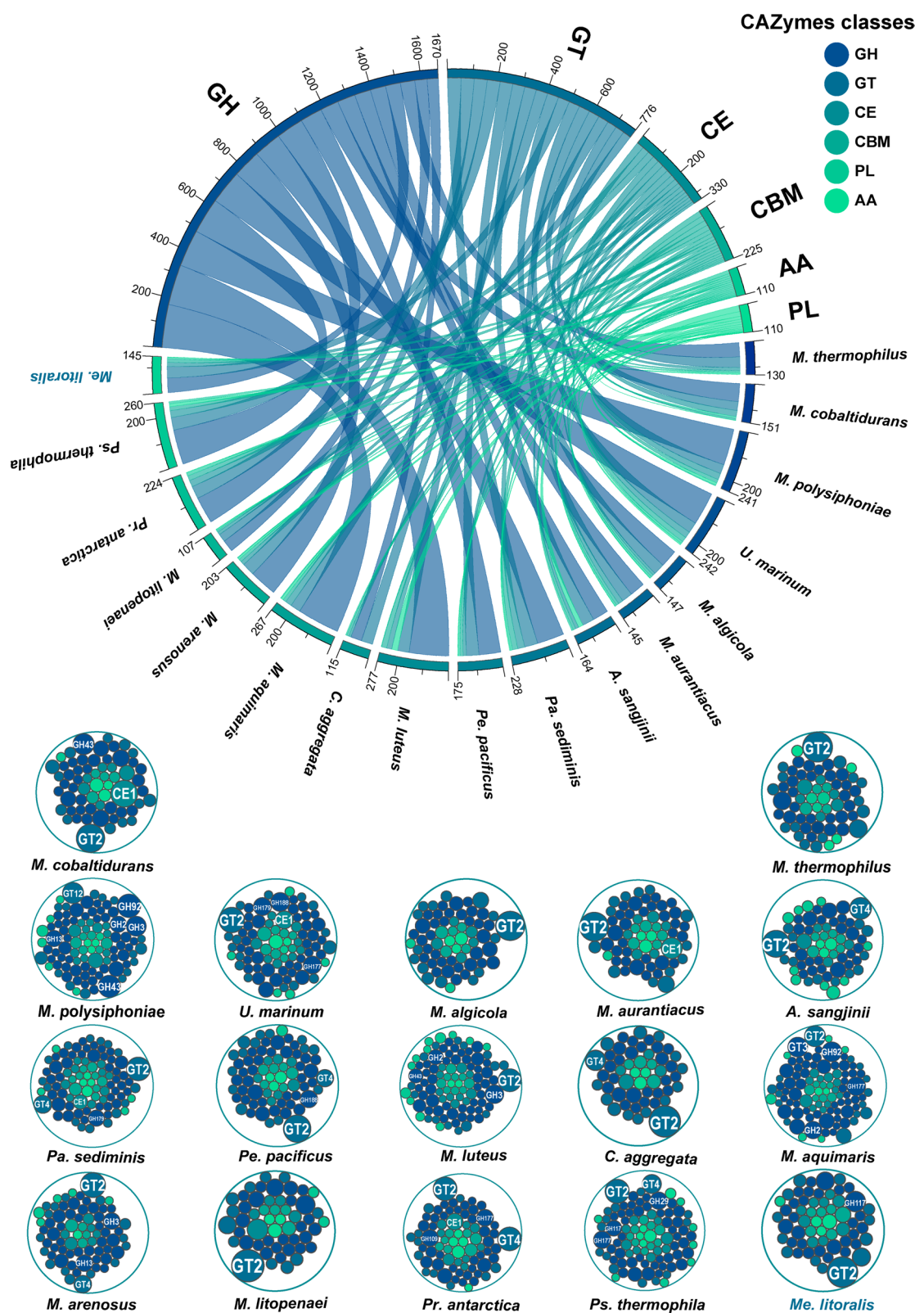


**Fig. 7** (See legend on previous page.)



CE enzymes release acyl or alkyl groups attached by ester linkage to carbohydrates and facilitate the degradation of complex polysaccharides [96], such as pectin and alginate [97]. Among the CE families identified in the genomes of strain NBU2967<sup>T</sup> and reference strains within the family *Flavobacteriaceae*, CE1 and CE14 were the most abundant (Table S3). These two families represent some of the largest and most diverse groups of CE enzymes, predominantly of bacterial origin [98]. They are recognized for facilitating the degradation of xylan, a component of plant cell walls, and chitin, a constituent of crustacean shells, respectively [98, 99]. It is presumed that strain NBU2967<sup>T</sup> could utilize CE1 enzymes to facilitate the hydrolysis of recalcitrant polysaccharides.

CBM enzymes are frequently associated with catalytic CAZymes and enhance their activity by binding to various carbohydrates [100]. Among the CBM families identified, CBM9 was the most abundant in the genomes of strain NBU2967<sup>T</sup> and reference strains within the family *Flavobacteriaceae* (Table S3). CBM9 proteins play a crucial role in the degradation of xylan [101].

PL enzymes cleave uronic acid-containing polysaccharides through a  $\beta$ -elimination mechanism, in contrast to the hydrolysis mechanism used by most other CAZymes [102]. This distinctive catalytic strategy allows PL enzymes to degrade a broader range of polysaccharides. Among the PL families identified in the genomes of strain NBU2967<sup>T</sup> and reference strains within the family *Flavobacteriaceae*, PL1, PL6, and PL7 were the most abundant (Table S3). These enzymes are crucial in breaking down polysaccharides derived from phytoplankton, such as alginate and pectin [103, 104]. This suggests that strain NBU2967<sup>T</sup> may be particularly adapted to degrade algal polysaccharides. Previous studies have shown that *Flavobacteriaceae* strains are efficient in utilizing high-molecular-weight compounds released by phytoplankton, converting these compounds into CO<sub>2</sub> or bacterial biomass, which is subsequently incorporated into the marine food web [105]. This bacterial-mediated process is vital for the turnover of phytoplankton-derived organic carbon, influencing carbon flow within marine ecosystems and contributing to the global carbon cycle.

AA3 enzymes were the most abundant AA family identified in the genomes of strain NBU2967<sup>T</sup> and reference strains within the family *Flavobacteriaceae* (Table S3). AA3, which consist of four subfamilies (AA3\_1, AA3\_2, AA3\_3, AA3\_4), assists in lignocellulose degradation with its reaction products [106].

In summary, the abundant CAZymes identified in strain NBU2967<sup>T</sup> and reference strains within the family *Flavobacteriaceae* suggests that they have a great potential for utilizing marine-derived polysaccharides.

### Prediction of secondary metabolites

Analysis of the predicted secondary metabolites from strain NBU2967<sup>T</sup> and reference strains within the family *Flavobacteriaceae* revealed a remarkable diversity and varying degrees of ubiquity in their biosynthetic pathways. Metabolites such as terpenes and aryl polyenes were detected in almost all strains (Fig. S9). As raw materials, terpenoids are extensively used in the pharmaceutical industry due to their antitumor, anti-inflammatory, antibacterial, antiviral, and antimalarial properties [107]. In contrast, secondary metabolite pathways such as non-ribosomal peptide synthetases (NRPS) and type III polyketide synthases (T3PKS) were identified only in a subset of strains. T3PKS are versatile enzymes involved in the biosynthesis of polyketides, which are secondary metabolites with diverse biological activities, including antimicrobial, antifungal, and anticancer properties [108]. This metabolic diversity highlights the potential ecological roles of strain NBU2967<sup>T</sup> and reference strains within the family *Flavobacteriaceae* in marine ecosystems.

### Pangenome analysis

For strain NBU2967<sup>T</sup> and all reference strains, the pangenome contains 29,364 genes, of which the core genome represents 863 genes (approximately 2.9%), whereas the shell and unique genes represent 7,596 (approximately 25.9%) and 20,905 genes (approximately 71.2%), respectively. The number of core genes, shared genes, and unique genes in each strain is shown in Table S4. The remarkably low number of core genes in strain NBU2967<sup>T</sup> and reference strains within the family *Flavobacteriaceae* suggests that these microorganisms have

(See figure on next page.)

**Fig. 8** Pangenome analysis of strain NBU2967<sup>T</sup> and reference strains. **(A)**, Clustering of genomes based on the presence/absence patterns of 29,364 pangenomic genes; **(B)**, Pan and core genome sizes. Blue is pan genome size and red is core genome size. The numbers of pan and core genes are plotted as a function of the number of genomes (g) added sequentially. y-axis shows the change in core genome and pan genome sizes as a function of random addition of genomes plotted on x-axis. The sizes of core and pan genomes were computed using OMCL algorithm. The best fit regression represents the Tettelin curve for both core and pan genomes. CL, completeness. CN, contigs. GN, gene number. GL, genome length

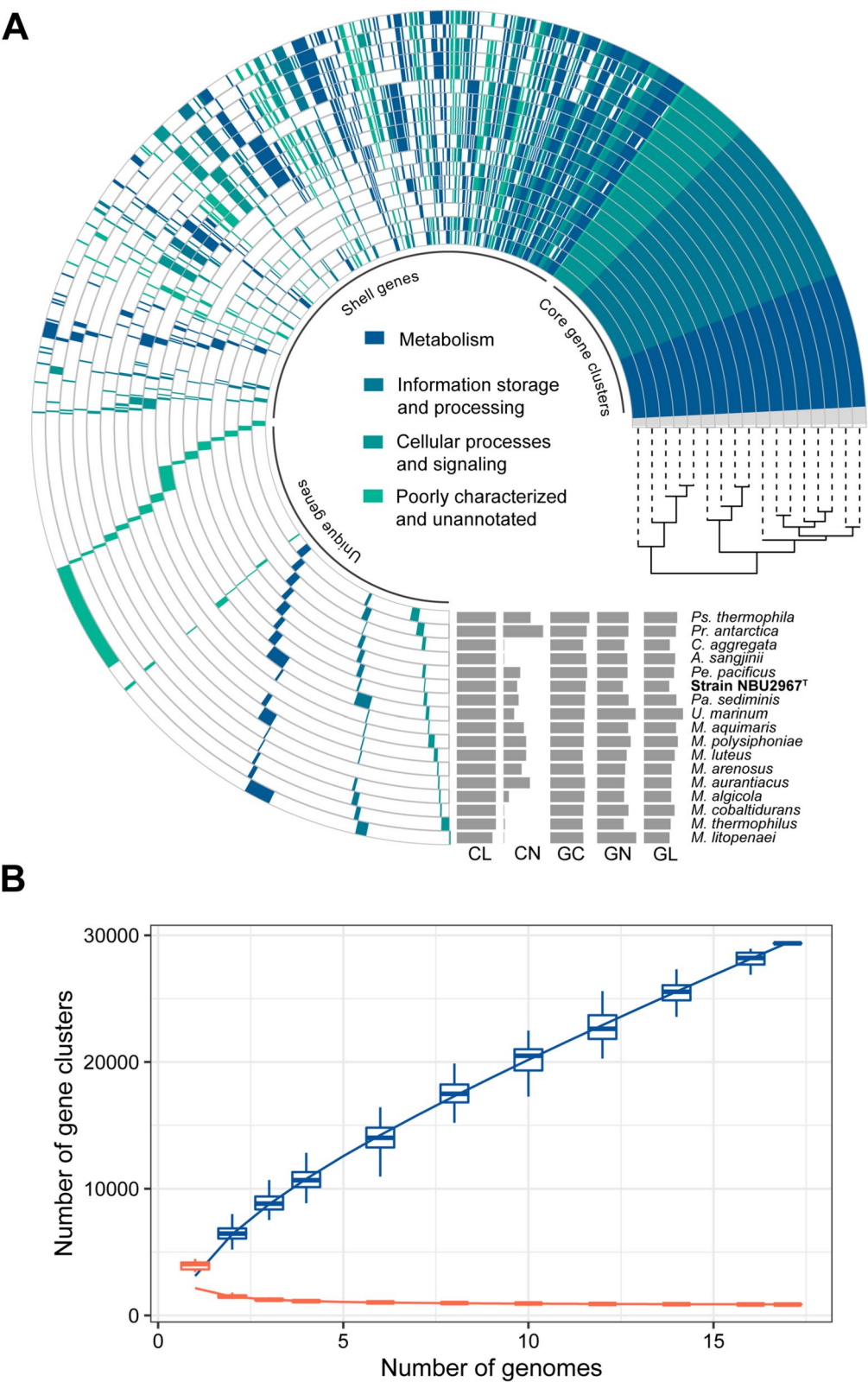


**Fig. 8** (See legend on previous page.)

undergone extensive horizontal gene transfer and gene loss events, resulting in highly distinct genetic compositions among different strains. This pronounced genetic diversity is likely a key factor in their ecological adaptability. Additionally, the substantial diversity of unique genes likely enhances the competitive fitness of individual strains within specific ecological niches [109]. This indicates a high degree of genetic diversity and some

level of conservation in the genomes of strain NBU2967<sup>T</sup> and reference strains within the family *Flavobacteriaceae* (Fig. 8A). As shown by the Tettelin bets ft. curve (Fig. 8B), the increase in pangenome size was indeterminate until the accession of the last genome, so the pangenome of strain NBU2967<sup>T</sup> and reference strains within the family *Flavobacteriaceae* may be classified as ‘open’ for expansion.

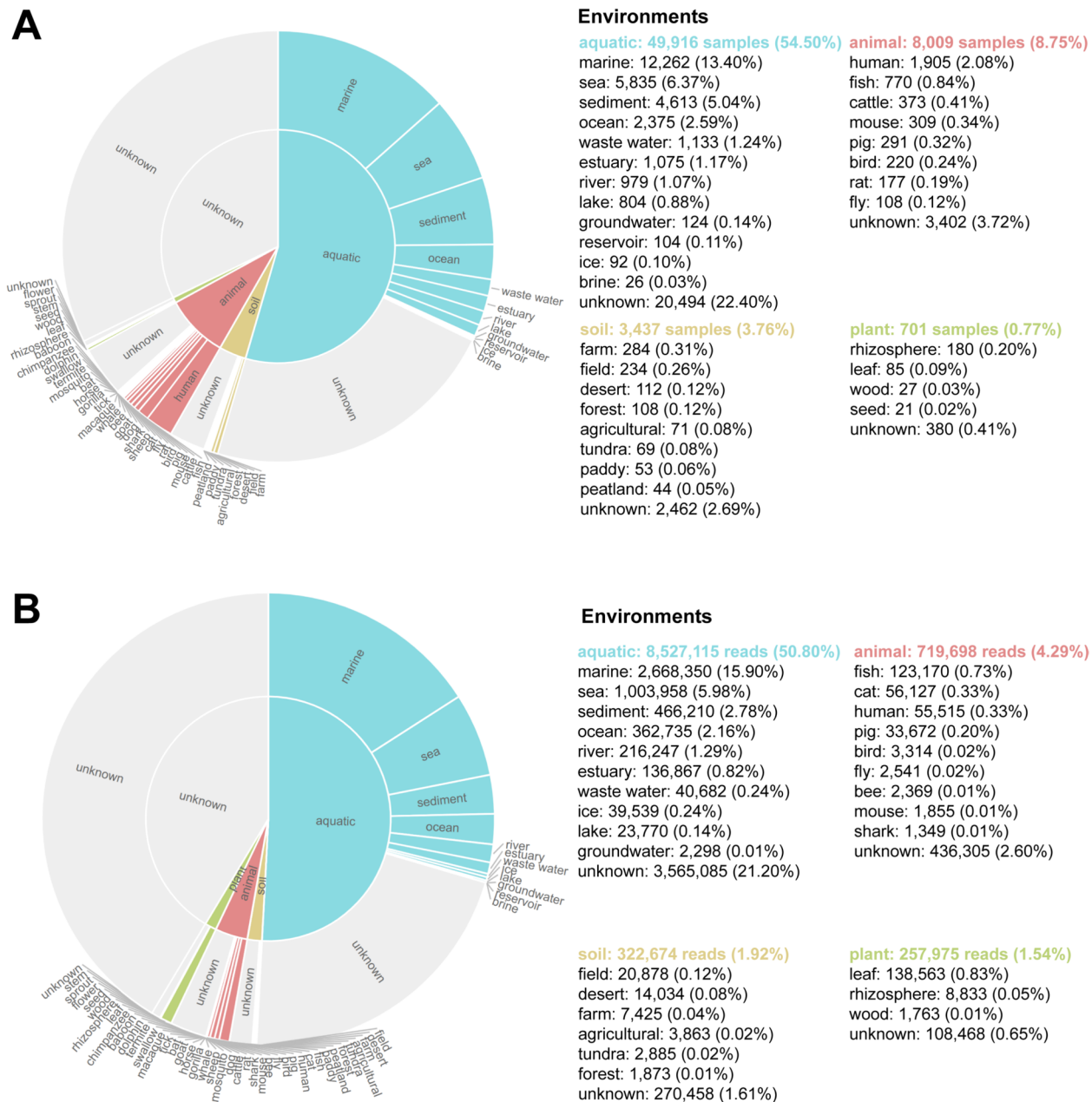


**Fig. 9** Biogeographic distribution analysis of the newly described genus *Meishania*. **(A)**, Frequency of samples with representative OTU sequence, by habitat and sub-habitat; **(B)**, Abundance of sequencing reads mapping to the representative OTU sequence, by habitat and sub-habitat

### Environmental distribution of the newly described genus *Meishania*

The MAP database was used to determine the world-wide distribution of the newly described genus *Meishania*. A total of 91,531 samples from 8,164 projects were analyzed to identify the representative sequence. The results of the biogeographic distribution analysis indicated that genus *Meishania* is widespread across different habitats, including aquatic, soil, animal, and plant environments. Specifically, genus *Meishania* were found in 49,916 aquatic samples (54.4%), 8,009 animal samples (8.8%), 3,437 soil samples (3.8%), and 701 plant samples (0.8%). Among the known environments, the primary habitats for genus *Meishania* were identified as the marine environment (22.4%) (Fig. 9A). The mapping of database sequencing reads to the standard operational taxonomic unit (OTU) sequence also showed that the marine environment had a predominant proportion (24.0%) of reads from the genus *Meishania* (Fig. 9B).

This distribution suggests that genus *Meishania* may play an important role in aquatic ecosystems, especially in the oceans, and may be associated with specific ecological adaptations and environmental conditions in the waters. Given the detection of sequences in plant- and animal-associated samples, there is also potential for symbiotic or opportunistic interactions, which merits further investigation.

### Conclusion

This study offers a thorough taxonomic, genomic, and ecological analysis of a novel *Flavobacteriaceae* strain, NBU2967<sup>T</sup>, isolated from coastal tidal flats. Phylogenetic analysis demonstrates that this strain represents a new genus within the *Flavobacteriaceae* family, with its genome sequence exhibiting significant divergence from closely related species. Genomic characterization reveals distinct metabolic pathways that enable NBU2967<sup>T</sup> to efficiently degrade a wide range of organic carbon sources, particularly marine polysaccharides, such as alginate and plant cell wall components. This highlights the strain's pivotal role in carbon cycling within tidal flat ecosystems. Additionally, environmental distribution analysis shows that newly described genus *Meishania* is widely distributed across global aquatic environments, particularly marine ecosystems. Collectively, these findings provide novel insights into the ecological functions of *Flavobacteriaceae* strains in tidal flat ecosystems and their potential role in organic matter degradation.

### Description of *Meishania* gen. nov.

*Meishania* (Mei.sha'ni.a. N.L. fem. n. *Meishania*, named for Meishan Island, the location where the bacterium was first isolated).

Cells are Gram-stain-negative, strictly aerobic, rod-shaped, and non-motile. Catalase- and oxidase-positive. The predominant menaquinone is MK-6. Major polar lipids are PE and APL. Major fatty acids are iso-C<sub>15:0</sub>, iso-C<sub>17:0</sub> 3-OH, and Summed Feature 1 (iso-C<sub>15:1</sub> H/C<sub>13:0</sub> 3-OH). The DNA G + C content of the type species is 42.5%. The type species is *Meishania litoralis*.

### Description of *Meishania litoralis* sp. nov.

*Meishania litoralis* (L. adj. litoralis, pertaining to the coast or shore, referring to its coastal sediment habitat).

Cells are Gram-stain-negative, strictly aerobic, rod-shaped, and non-flagellated, measuring 0.6–0.8 µm in width and 1.2–1.6 µm in length. Colonies are circular, elevated, smooth, and orange-yellow, reaching up to 1 mm in diameter after 48 h of incubation on MA medium at 37°C. Growth occurs at pH 5.5–8.5 (optimum pH 6.5), temperatures ranging from 10°C to 40°C (optimum 37°C), and NaCl concentrations of 1–5% (optimum 2%). The cells are positive for catalase, oxidase, the methyl red test, and hydrolysis of Tweens 20, 40, 60, and 80. They are negative for H<sub>2</sub>S production, the Voges-Proskauer test, and hydrolysis of starch and casein. Fatty acids (> 10%) include iso-C<sub>15:0</sub>, iso-C<sub>17:0</sub> 3-OH, and Summed Feature 1 (iso-C<sub>15:1</sub> H/C<sub>13:0</sub> 3-OH). The sole respiratory quinone is MK-6. Polar lipids include PE, APL, two unidentified Ls, two unidentified PLs, and three unidentified ALs.

The type strain, NBU2967<sup>T</sup> (= KCTC 82912<sup>T</sup> = MCCC 1 K06391<sup>T</sup>), was isolated from the unvegetated tidal flats of Meishan Island in the East China Sea. The GenBank/EMBL/DBJ accession numbers for the 16S rRNA gene sequence and draft genome sequence of the strain are MZ025914 and JBHFPV000000000, respectively.

### Abbreviations

CAZyme	Carbohydrate-active enzyme
PUL	Polysaccharide utilization loci
MA	Marine agar 2216
MB	Marine broth 2216
FAME	Fatty acid methyl ester
MIDI	Microbial identification system
HPLC-MS	High-performance liquid chromatography-mass spectrometry
TLC	Thin layer chromatography
CDS	Coding sequence
RAST	Rapid annotation using subsystem technology
ORF	Open reading frames
ANI	Average nucleotide identity
AAI	Average amino acid identity
dDDH	Digital DNA-DNA hybridization
GGDC	Genome-to-genome distance calculator
TYGS	Type strain genome server
BGC	Biosynthetic gene clusters
MAP	Microbe atlas project
PE	Phosphatidylethanolamine
APL	Aminophospholipid
L	Lipid
PL	Phospholipid
AL	Amido lipid
GABA	Gamma-aminobutyric acid
PAPS	Phosphoadenosine phosphosulfate



RMSD	Root mean square deviation
GH	Glycoside hydrolase
GT	Glycosyltransferase
CE	Carbohydrate esterase
CBM	Carbohydrate binding module
AA	Auxiliary activities
PL	Polysaccharide lyase
NRPS	Non-ribosomal peptide synthetases
T3PKS	Type III polyketide synthases
OUT	Operational taxonomic unit

## Supplementary Information

The online version contains supplementary material available at <https://doi.org/10.1186/s12866-025-04069-2>.

Supplementary Material 1.

## Acknowledgements

We are deeply grateful to Professor Shan He and Associate Researcher Weiyan Zhang for their invaluable contributions to data analysis and financial support throughout this research endeavor.

## Authors' contributions

WHH: Conceptualization, Data curation, Formal analysis, Investigation, Methodology, Software, Visualization, Writing – original draft. LJH: Data curation, Writing – review & editing. GYF: Data curation, Writing – review & editing. CYQ: Data curation, Writing – review & editing. ZC: Data curation, Writing – review & editing. DLJ: Supervision, Validation, Writing – review & editing. HS: Conceptualization, Funding acquisition, Supervision, Validation, Writing – review & editing. ZWY: Conceptualization, Funding acquisition, Project administration, Writing – review & editing.

## Funding

This work was supported by the National Natural Science Foundation of China (42176101), the Ningbo Key Science and Technology Development Program (2021Z046), the Scientific Research Foundation of Graduate School of Ningbo University (IF2021087), the National 111 Project of China (D16013) and the Li Dak Sum Yip Yio Chin Kenneth Li Marine Biopharmaceutical Development Fund.

## Data availability

The GenBank/EMBL/DBJ accession numbers for the 16S rRNA gene sequence and draft genome sequence of strain NBU2967 T are MZ025914 and JBHFPV000000000, respectively.

## Declarations

### Ethics approval and consent to participate

Not applicable.

### Consent for publication

Not applicable.

### Competing interests

The authors declare no competing interests.

### Author details

<sup>1</sup>College of Food Science and Engineering, Ningbo University, Ningbo 315800, P. R. China. <sup>2</sup>Li Dak Sum Yip Yio Chin Kenneth Li Marine Biopharmaceutical Research Center, Ningbo University, Ningbo 315800, P. R. China. <sup>3</sup>Ningbo Institute of Marine Medicine, Peking University, Ningbo 315800, P. R. China.

Received: 8 April 2025 Accepted: 22 May 2025

Published online: 30 May 2025

## References

- Yang S, Park HS, Kwon BO, Khim JS, Lee J, Shares G, et al. Assessing the contribution of Tidal Flats to climate change and carbon neutrality through modeling approaches. *Mar Environ Res*. 2025;207:107067. <https://doi.org/10.1016/j.marenvres.2025.107067>.
- Gómez-Consarnau L, Needham DM, Weber PK, Fuhrman JA, Mayali X. Influence of light on particulate organic matter utilization by attached and free-living marine bacteria. *Front Microbiol*. 2019;2019(10):1204. <https://doi.org/10.3389/fmicb.2019.01204>.
- Seo H, Kim JH, Lee SM, Lee SW. The Plant-Associated *Flavobacterium*: a hidden helper for improving plant health. *Plant Pathol J*. 2024;40(3):251–60. <https://doi.org/10.5423/ppj.Rw.01.2024.0019>.
- Hameed A, Lai W-A, Shahina M, Stothard P, Young L-S, Lin S-Y, Sridhar KR, Young C-C. Differential visible spectral influence on carbon metabolism in heterotrophic marine *flavobacteria*. *FEMS Microbiol Ecol*. 2020;96(3):fiaa011. <https://doi.org/10.1093/femsec/fiaa011>.
- Lian X-D, Guan Y, Jiang Y, Kwak D-H, Lee M-K, Li Z. Discovery of two novel *Flavobacterium* species with potential for complex polysaccharide degradation. *Sci Rep*. 2025;15(1):3494. <https://doi.org/10.1038/s41598-025-87876-x>.
- Gong B, Cao H, Peng C, Perčulija V, Tong G, Fang, et al. High-throughput sequencing and analysis of microbial communities in the mangrove swamps along the coast of Beibu Gulf in Guangxi. *China Sci Rep*. 2019;9(1):9377. <https://doi.org/10.1038/s41598-019-45804-w>.
- Rinke M, Maraun M, Scheu S. Spatial and temporal variations in salt marsh microorganisms of the Wadden Sea. *Ecol Evol*. 2022;12(3):e8767. <https://doi.org/10.1002/ece3.8767>.
- Zhang R, Sun M, Zhang H, Zhao Z. Spatial separation of microbial communities reflects gradients of salinity and temperature in offshore sediments from Shenzhen, south China. *Ocean Coast Manag*. 2021;214:105904. <https://doi.org/10.1016/j.ocecoaman.2021.105904>.
- Reichenbach H. "The Order Cytophagales," in *The Prokaryotes: A Handbook on the Biology of Bacteria: Ecophysiology, Isolation, Identification, Applications*, eds. A. Balows, H.G. Trüper, M. Dworkin, W. Harder & K.-H. Schleifer. (New York, NY: Springer New York). 1992;3631–3675. [https://doi.org/10.1007/978-1-4757-2191-1\\_37](https://doi.org/10.1007/978-1-4757-2191-1_37).
- Bernardet JF, Segers P, Vancannet M, Berthe F, Kersters K, Vandamme P. Cutting a Gordian Knot: Emended Classification and Description of the Genus *Flavobacterium*, Emended Description of the Family *Flavobacteriaceae*, and Proposal of *Flavobacterium hydatidis* nom. nov. (Basionym, *Cytophaga aquatilis* Strohl and Tait 1978). 1996;46(1):128–148. <https://doi.org/10.1099/00207713-46-1-128>.
- Bernardet J.-F.; Nakagawa Y.; Holmes B.; Subcommittee on the taxonomy of Flavobacterium and Cytophaga-like bacteria of the International Committee on Systematics of Prokaryotes. Proposed minimal standards for describing new taxa of the family *Flavobacteriaceae* and emended description of the family. *Int J Syst Evol Microbiol*. 2002;52(3):1049–70. <https://doi.org/10.1099/00207713-52-3-1049>.
- García-López M, Meier-Kolthoff JP, Tindall BJ, Gronow S, Woyke T, Kyrpides NC, et al. Analysis of 1,000 Type-Strain Genomes Improves Taxonomic Classification of Bacteroidetes. 2019;10. <https://doi.org/10.3389/fmicb.2019.02083>.
- Parte AC, Sardà Carbasse J, Meier-Kolthoff JP, Reimer LC, Göker M. List of Prokaryotic names with Standing in Nomenclature (LPSN) moves to the DSMZ. *Int J Systematic Evol Microbiol*. 2020;70(11):5607–12. <https://doi.org/10.1099/ijsem.0004332>.
- Williams TJ, Wilkins D, Long E, Evans F, DeMaere MZ, Raftery MJ, Cavicchioli R. The role of planktonic *Flavobacteria* in processing algal organic matter in coastal East Antarctica revealed using metagenomics and metaproteomics. *Environ Microbiol*. 2013;15(5):1302–17. <https://doi.org/10.1111/1462-2920.12017>.
- Pontiller B, Martínez-García S, Joglar V, Amnebrink D, Pérez-Martínez C, González JM, Lundin D, Fernández E, Teira E, Pinhassi J. Rapid bacterioplankton transcription cascades regulate organic matter utilization during phytoplankton bloom progression in a coastal upwelling system. *ISME J*. 2022;16(10):2360–72. <https://doi.org/10.1038/s41396-022-01273-0>.
- Moran MA, Kujawinski EB, Schroer WF, Amin SA, Bates NR, Bertrand EM, et al. Microbial metabolites in the marine carbon cycle. *Nat Microbiol*. 2022;7(4):508–23. <https://doi.org/10.1038/s41564-022-01090-3>.

17. Giordano D, Coppola D, Russo R, Denaro R, Giuliano L, Lauro FM, et al. "Chapter Four - Marine Microbial Secondary Metabolites: Pathways, Evolution and Physiological Roles," in *Adv. Microb. Physiol.*, ed. R.K. Poole. Academic Press. 2015;357–428. <https://doi.org/10.1016/b.s.ampbs.2015.04.001>.
18. Tripathi N, Sapra A. Gram Staining. Treasure Island (FL): StatPearls Publishing; 2023.
19. Xu X-W, Wu M, Zhou P-J, Liu S-J. *Halobiforma laticalsi* sp. nov., isolated from a salt lake in China. *Int J Syst Evol Microbiol.* 2005;55(5):1949–52. <https://doi.org/10.1099/ijs.0.63742-0>.
20. Zhang W, Zhu S, Cheng Y, Ding L, Li S, Peng N, He S. *Rheinheimera mangrovi* sp. nov., a bacterium isolated from mangrove sediment. *Int J Syst Evol Microbiol.* 2020;70(12):6188–94. <https://doi.org/10.1099/ijsem.0.004513>.
21. Wu Y-H, Xu L, Zhou P, Wang C-S, Oren A, Xu X-W. *Brevirhabdus pacifica* gen. nov., sp. nov., isolated from deep-sea sediment in a hydrothermal vent field. *Int J Syst Evol Microbiol.* 2015;65(10):3645–51. <https://doi.org/10.1099/ijsem.0.000469>.
22. Minnikin DE, O'Donnell AG, Goodfellow M, Alderson G, Athalye M, Schaal A, et al. An integrated procedure for the extraction of bacterial isoprenoid quinones and polar lipids. *J Microbiol Methods.* 1984;2(5):233–41. [https://doi.org/10.1016/0167-7012\(84\)90018-6](https://doi.org/10.1016/0167-7012(84)90018-6).
23. Zhang X-Q, Sun C, Wang C-S, Zhang X, Zhou X, Wu Y-H, et al. *Sinimaribacterium flocculans* gen. nov., sp. nov., a gammaproteobacterium from offshore surface seawater. *Int J Syst Evol Microbiol.* 2015;65(Pt-10):3541–6. <https://doi.org/10.1099/ijsem.0.000452>.
24. Sun C, Wu C, Su Y, Wang R-J, Fu G-Y, Zhao Z, et al. *Hyphococcus flavus* gen. nov., sp. nov., a novel alphaproteobacterium isolated from deep seawater. *Int J Syst Evol Microbiol.* 2017;67(10):4024–31. <https://doi.org/10.1099/ijsem.0.002237>.
25. Yoon S-H, Ha S-M, Kwon S, Lim J, Kim Y, Seo H, et al. Introducing EzBioCloud: a taxonomically united database of 16S rRNA gene sequences and whole-genome assemblies. *Int J Syst Evol Microbiol.* 2017;67(5):1613–7. <https://doi.org/10.1099/ijsem.0.001755>.
26. Lam-Tung N, Schmidt HA, von Haeseler A, Bui Quang M. IQ-TREE: a fast and effective stochastic algorithm for estimating maximum-likelihood phylogenies. *Mol Biol Evol.* 2015;32(1):268–74. <https://doi.org/10.1093/molbev/msu300>.
27. Saitou N, Nei M. The neighbor-joining method: a new method for reconstructing phylogenetic trees. *Mol Biol Evol.* 1987;4(4):406–25. <https://doi.org/10.1093/oxfordjournals.molbev.a040454>.
28. Fitch WM. Toward defining the course of evolution: minimum change for a specific tree topology. *Syst Biol.* 1971;20(4):406–16. <https://doi.org/10.1093/sysbio/20.4.406>.
29. Felsenstein J. Evolutionary trees from DNA sequences: a maximum likelihood approach. *J Mol Evol.* 1981;17(6):368–76. <https://doi.org/10.1007/bf01734359>.
30. Kimura M. A simple method for estimating evolutionary rates of base substitutions through comparative studies of nucleotide sequences. *J Mol Evol.* 1980;16(2):111–20. <https://doi.org/10.1007/bf01731581>.
31. Khan SA, Jeong SE, Baek JH, Jeon CO. *Maribacter algicola* sp. nov., isolated from a marine red alga, *Porphyridium marinum*, and transfer of *Maripseudobacter aurantiacus* Chen et al. 2017 to the genus *Maribacter* as *Maribacter aurantiacus* comb. Nov. *Int J Syst Evol Microbiol.* 2020;70(2):797–804. <https://doi.org/10.1099/ijsem.0.003828>.
32. Nedashkovskaya OI, Kim SB, Han SK, Lysenko AM, Rohde M, Rhee M-S, Frolova GM, Falsen E, Mikhailov VV, Bae KS. *Maribacter* gen. nov., a new member of the family Flavobacteriaceae, isolated from marine habitats, containing the species *Maribacter sedimenticola* sp. nov., *Maribacter aquivivus* sp. nov., *Maribacter orientalis* sp. nov. and *Maribacter ulvicola* sp. nov. *Int J Syst Evol Microbiol.* 2004;54(4):1017–23. <https://doi.org/10.1099/ijs.0.02849-0>.
33. Chung D, Jung J, Kim JYH, Kim KW, Kwon YM. *Aggregatimonas sangjinii* gen. nov., sp. nov., a novel silver nanoparticle synthesizing bacterium belonging to the family Flavobacteriaceae. *Antonie Leeuwenhoek.* 2022;115(2):325–35. <https://doi.org/10.1007/s10482-021-01700-w>.
34. Kwon KK, Lee YK, Lee HK. *Costertonia aggregata* gen. nov., sp. nov., a mesophilic marine bacterium of the family Flavobacteriaceae, isolated from a mature biofilm. *Int J Syst Evol Microbiol.* 2006;56(6):1349–53. <https://doi.org/10.1099/ijs.0.64168-0>.
35. Zhang Z, Hu Z, Tang L, Wang Z, Zhang Y. *Ulvibacterium marinum* gen. nov., sp. nov., a novel marine bacterium of the family Flavobacteriaceae, isolated from a culture of the green alga *Ulva prolifera*. *Antonie Leeuwenhoek.* 2019;112(7):1077–85. <https://doi.org/10.1007/s10482-019-01239-x>.
36. Nedashkovskaya OI, Suzuki M, Lee J-S, Lee KC, Shevchenko LS, Mikhailov VV. *Pseudozobellia thermophila* gen. nov., sp. nov., a bacterium of the family Flavobacteriaceae, isolated from the green alga *Ulva fenestrata*. *Int J Syst Evol Microbiol.* 2009;59(4):806–10. <https://doi.org/10.1099/ijs.0.004143-0>.
37. Huang Z, Wei X, Lai Q, Chen S, Yuan J. *Pareuzebyella sediminis* gen. nov., sp. nov., a novel marine bacterium in the family Flavobacteriaceae, isolated from a tidal flat sediment. *Int J Syst Evol Microbiol.* 2020;71(1):004606. <https://doi.org/10.1099/ijsem.0.004606>.
38. Li R, Li Y, Kristiansen K, Wang J. SOAP: short oligonucleotide alignment program. *Bioinformatics.* 2008;24(5):713–4. <https://doi.org/10.1093/bioinformatics/btn025>.
39. Seemann T. Prokka: Rapid prokaryotic genome annotation. *Bioinformatics.* 2014;30(14):2068–9. <https://doi.org/10.1093/bioinformatics/btu153>.
40. Hyatt D, Chen G-L, LoCascio PF, Land ML, Larimer FW, Hauser LJ. Prodigal: prokaryotic gene recognition and translation initiation site identification. *BMC Bioinformatics.* 2010;11(1):119. <https://doi.org/10.1186/1471-2105-11-119>.
41. Lagesen K, Hallin P, Rødland EA, Stærfeldt HH, Rognes T, Ussery DW. RNAmmer: Consistent and rapid annotation of ribosomal RNA genes. *Nucleic Acids Res.* 2007;35(9):3100–8. <https://doi.org/10.1093/nar/gkm160>.
42. Laslett D, Canback B. ARAGORN, a program to detect tRNA genes and tmRNA genes in nucleotide sequences. *Nucleic Acids Res.* 2004;32(1):11–6. <https://doi.org/10.1093/nar/gkh152>.
43. Petersen TN, Brunak S, Von Heijne G, Nielsen H. SignalP 4.0: Discriminating signal peptides from transmembrane regions. *Nat Meth.* 2011;8(10):785–6. <https://doi.org/10.1038/nmeth.1701>.
44. Kolbe DL, Eddy SR. Fast filtering for RNA homology search. *Bioinformatics.* 2011;27(22):3102–9. <https://doi.org/10.1093/bioinformatics/btr545>.
45. Overbeek R, Olson R, Pusch GD, Olsen GJ, Davis JJ, Disz T, et al. The SEED and the Rapid Annotation of microbial genomes using Subsystems Technology (RAST). *Nucleic Acids Res.* 2014;42(D1):D206–14. <https://doi.org/10.1093/nar/gkt1226>.
46. Kanehisa M, Sato Y, Morishima K. BlastKOALA and GhostKOALA: KEGG tools for functional characterization of genome and metagenome sequences. *J Mol Biol.* 2016;428(4):726–31. <https://doi.org/10.1016/j.jmb.2015.11.006>.
47. Fang C, Wu Y-H, Xamxidini M, Wang C-S, Xu X-W. *Maribacter cobaltidurans* sp. nov., a heavy-metal-tolerant bacterium isolated from deep-sea sediment. *Int J Syst Evol Microbiol.* 2017;67(12):5261–7. <https://doi.org/10.1099/ijsem.0.002458>.
48. Chen C, Su Y, Tao T, Fu G, Zhang C, Sun C, et al. *Maripseudobacter aurantiacus* gen. nov., sp. nov., a novel member of the family Flavobacteriaceae isolated from a sedimentation basin. *Int J Syst Evol Microbiol.* 2017;67(4):778–83. <https://doi.org/10.1099/ijsem.0.001580>.
49. Tang M, Wang G, Xiang W, Chen C, Wu J, Dai S, et al. *Maribacter flavus* sp. nov., isolated from a cyanobacterial culture pond. *Int J Syst Evol Microbiol.* 2015;65(Pt\_11):3997–4002. <https://doi.org/10.1099/ijsem.0.000526>.
50. Thongphrom C, Kim J-H, Kim W. *Maribacter arenosus* sp. nov., isolated from marine sediment. *Int J Syst Evol Microbiol.* 2016;66(11):4826–31. <https://doi.org/10.1099/ijsem.0.001436>.
51. Kim SY, Choi JY, Hong YW, Shin DY, Kim BJ, Kang JK, et al. *Maribacter litopenaei* sp. nov., isolated from the intestinal tract of the Pacific white shrimp *Litopenaeus vannamei*. *Int J Syst Evol Microbiol.* 2023;73(3):005786. <https://doi.org/10.1099/ijsem.0.005786>.
52. Hu J, Yang QQ, Ren Y, Zhang WW, Zheng G, Sun C, et al. *Maribacter thermophilus* sp. nov., isolated from an algal bloom in an intertidal zone, and emended description of the genus *Maribacter*. *Int J Syst Evol Mol.* 2015;65(Pt\_1):36–41. <https://doi.org/10.1099/ijs.0.064774-0>.
53. Yu Y, Li HR, Zeng YX, Sun K, Chen B. *Prisia antarctica* gen. nov., sp. nov., a member of the family Flavobacteriaceae, isolated from Antarctic intertidal sediment. 2012;62(Pt\_9), 2218–2223. <https://doi.org/10.1099/ijs.0.037515-0>.

54. Wang Q, Liu F, Zhang DC. *Pelagihabitans pacificus* gen. nov., sp. nov., a member of the family *Flavobacteriaceae* isolated from a deep-sea seamount. 2020;70(8):4569–4575. <https://doi.org/10.1099/ijsem.0.004315>.
55. Liu A, Zhang YJ, Liu DK, Li XZ. *Maribacter luteus* sp. nov., a marine bacterium isolated from intertidal sand of the Yellow Sea. 2020;70(5):3497–3503. <https://doi.org/10.1099/ijsem.0.004206>.
56. Zhang Y, Zhai Y, Mu L, Hu M, Fang W, Xiao Y, et al. *Maribacter aquimaris* sp. nov., isolated from seawater adjacent to Fildes Peninsula, Antarctica. Antonie Leeuwenhoek. 2023;116(8):753–761. <https://doi.org/10.1007/s10482-023-01844-x>.
57. Nedashkovskaya OI, Vancanneyt M, De Vos P, Kim SB, Lee MS, Mikhailov VV. *Maribacter polysiphoniae* sp. nov., isolated from a red alga. 2007;57(12):2840–2843. <https://doi.org/10.1099/ijms.0.65181-0>.
58. Yoon S-H, Ha S-M, Lim J, Kwon S, Chun J. A large-scale evaluation of algorithms to calculate average nucleotide identity. Antonie Leeuwenhoek. 2017;110(10):1281–6. <https://doi.org/10.1007/s10482-017-0844-4>.
59. Kim D, Park S, Chun J. Introducing EZAAI: a pipeline for high throughput calculations of prokaryotic average amino acid identity. J Microbiol. 2021;59(5):476–80. <https://doi.org/10.1007/s12275-021-1154-0>.
60. Meier-Kolthoff JP, Auch AF, Klenk HP, Goekoe M. Genome sequence-based species delimitation with confidence intervals and improved distance functions. BMC Bioinformatics. 2013;14. <https://doi.org/10.1186/1471-2105-14-60>.
61. Meier-Kolthoff JP, Göker M. TYGS is an automated high-throughput platform for state-of-the-art genome-based taxonomy. Nat Commun. 2019;10(1):2182. <https://doi.org/10.1038/s41467-019-10210-3>.
62. Riesco R, Trujillo ME. Update on the proposed minimal standards for the use of genome data for the taxonomy of prokaryotes. 2024;74(3). <https://doi.org/10.1099/ijsem.0.006300>.
63. Zheng J, Ge Q, Yan Y, Zhang X, Huang L, Yin Y. DbCAN3: Automated carbohydrate-Active enzyme and substrate annotation. Nucleic Acids Res. 2023;51(W1):W115–21. <https://doi.org/10.1093/nar/gkad328>.
64. Drula E, Garron M-L, Dogan S, Lombard V, Henrissat B, Terrapon N. The carbohydrate-active enzyme database: functions and literature. Nucleic Acids Res. 2022;50(D1):D571–7. <https://doi.org/10.1093/nar/gkab1045>.
65. Blin K, Shaw S, Steinke K, Villebro R, Ziemert N, Lee SY et al. antiSMASH 5.0: updates to the secondary metabolite genome mining pipeline. Nucleic Acids Res. 2019;47(W1):W81–w87. <https://doi.org/10.1093/nar/gkz310>.
66. Powell HR, Islam SA, David A, Sternberg MJE. Phyre2.2: A Community Resource for Template-based Protein Structure Prediction. J. Mol. Biol. 2025;168960. <https://doi.org/10.1016/j.jmb.2025.168960>.
67. van Kempen M, Kim SS, Tumescheit C, Mirdita M, Lee J, Gilchrist CLM, et al. Fast and accurate protein structure search with Foldseek. Nat Biotechnol. 2024;42(2):243–6. <https://doi.org/10.1038/s41587-023-01773-0>.
68. Zhang C, Shine M, Pyle AM, Zhang Y. US-align: universal structure alignments of proteins, nucleic acids, and macromolecular complexes. Nat Meth. 2022;19(9):1109–15. <https://doi.org/10.1038/s41592-022-01585-1>.
69. Tettelin H, Maignani V, Cieslewicz MJ, Donati C, Medini D, Ward NL, et al. Genome analysis of multiple pathogenic isolates of *Streptococcus agalactiae*: Implications for the microbial “pan-genome.” Proc Natl Acad Sci U S A. 2005;102(39):13950–5. <https://doi.org/10.1073/pnas.0506758102>.
70. Talwar C, Nagar S, Kumar R, Scaria J, Lal R, Negi RK. Defining the Environmental Adaptations of Genus *Devosia*: Insights into its Expansive Short Peptide Transport System and Positively Selected Genes. Sci Rep. 2020;10(1). <https://doi.org/10.1038/s41598-020-58163-8>.
71. Page AJ, Cummins CA, Hunt M, Wong VK, Reuter S, Holden MTG, et al. Roary: rapid large-scale prokaryote pan genome analysis. Bioinformatics. 2015;31(22):3691–3. <https://doi.org/10.1093/bioinformatics/btv421>.
72. Liu D, Zhang Y, Fan G, Sun D, Zhang X, Yu Z, et al. IPGA: A handy integrated prokaryotes genome and pan-genome analysis web service. iMeta. 2022;1(4). <https://doi.org/10.1002/imt2.55>.
73. Matias Rodrigues JF, Schmidt TSB, Tackmann J, von Mering C. MAPseq: highly efficient k-mer search with confidence estimates, for rRNA sequence analysis. Bioinformatics. 2017;33(23):3808–10. <https://doi.org/10.1093/bioinformatics/btx517>.
74. Chun J, Oren A, Ventosa A, Christensen H, Arahal DR, da Costa MS, et al. Proposed minimal standards for the use of genome data for the taxonomy of prokaryotes. 2018;68(1):461–6. <https://doi.org/10.1099/ijsem.0.002516>.
75. Konstantinidis KT, Rosselló-Móra R, Amann R. Uncultivated microbes in need of their own taxonomy. ISME J. 2017;11(11):2399–406. <https://doi.org/10.1038/ismej.2017.113>.
76. Barco RA, Garrity GM, Scott JJ, Amend JP, Nealson KH, Emerson D. A Genus Definition for Bacteria and Archaea Based on a Standard Genome Relatedness Index. mBio. 2020;11(1). <https://doi.org/10.1128/mbio.02475-19>.
77. Luo C, Rodriguez-R LM, Konstantinidis KT. MyTaxa: an advanced taxonomic classifier for genomic and metagenomic sequences. Nucleic Acids Res. 2014;42(8):e73–e73. <https://doi.org/10.1093/nar/gku169>.
78. Li M, Hou LZ, Xu XH, Wang XX, Zheng MC, Zhang YJ, et al. Phylogenomic Analyses of a Clade Within the Family *Flavobacteriaceae* Suggest Taxonomic Reassignments of Species of the Genera *Algibacter*, *Hyunsoonleella*, *Jejuia*, and *Flavivirga*, and the Proposal of *Pseudalgibacter* gen. nov. and *Pseudalgibacter alginicyticus* comb. nov. Curr. Microbiol. 2021;78(8):3277–3284. <https://doi.org/10.1007/s00284-021-02559-w>.
79. Wayne LG, Brenner DJ, Colwell RR, Grimont PAD, Kandler O, Krichevsky MI, et al. Report of the Ad Hoc Committee on Reconciliation of Approaches to Bacterial Systematics. 1987;37(4):463–4. <https://doi.org/10.1099/00207713-37-4-463>.
80. Yadav S, Koenen M, Bale NJ, Reitsma W, Engelmann JC, Stefanova K, Damsté JSS, Villanueva L. Organic matter degradation in the deep, sulfidic waters of the Black Sea: insights into the ecophysiology of novel anaerobic bacteria. Microbiome. 2024;12(1):98. <https://doi.org/10.1186/s40168-024-01816-x>.
81. Rashmi D, Zanan R, John S, Khandagale K, Nadaf A. Chapter 13 -  $\gamma$ -Aminobutyric Acid (GABA): Biosynthesis, Role, Commercial Production, and Applications. Stud Nat Prod Chem ed. R. Atta ur. Elsevier). 2018:413–452. <https://doi.org/10.1016/B978-0-444-64057-4.00013-2>.
82. Nurizzo D, Nagy T, Gilbert HJ, Davies GJ. The Structural Basis for Catalysis and Specificity of the *Pseudomonas cellulosa*  $\alpha$ -Glucuronidase, GlcA67A. Structure. 2002;10(4):547–56. [https://doi.org/10.1016/S0969-2126\(02\)00742-6](https://doi.org/10.1016/S0969-2126(02)00742-6).
83. Déjean G, Tamura K, Cabrera A, Jain N, Pudlo Nicholas A, Pereira G, et al. Synergy between Cell Surface Glycosidases and Glycan-Binding Proteins Dictates the Utilization of Specific Beta(1,3)-Glucans by Human Gut Bacteroides. mBio. 2020;11(2). <https://doi.org/10.1128/mbio.00095-00020>.
84. Etokakpan OU, Palmer GH. Comparative studies of the development of endosperm-degrading enzymes in maturing sorghum and barley. World J Microbiol Biotechnol. 1990;6(4):408–17. <https://doi.org/10.1007/BF01202124>.
85. Lisov AV, Belova OV, Belov AA, Lisova, ZA, Nagel AS, Shadrin AM, et al. Expression in *Pichia pastoris* of Thermostable Endo-1,4- $\beta$ -xylanase from the Actinobacterium *Nocardiopsis halotolerans*: Properties and Use for Saccharification of Xylan-Containing Products. Int J Mol Sci. 2024;25(16). <https://doi.org/10.3390/ijms25169121>.
86. Liu N, Kivenson V, Peng X, Cui Z, Lankiewicz Thomas S, Gosselin Kelsey M, et al. *Pontiella agarivorans* sp. nov., a novel marine anaerobic bacterium capable of degrading macroalgal polysaccharides and fixing nitrogen. Appl. Environ. Microbiol. 2024;90(2):e00914–00923. <https://doi.org/10.1128/aem.00914-23>.
87. Koprivova A, Schuck S, Jacoby RP, Klinkhammer I, Welter B, Leson L, et al. Root-specific camalexin biosynthesis controls the plant growth-promoting effects of multiple bacterial strains. Proc Natl Acad Sci U S A. 2019;116(31):15735–44. <https://doi.org/10.1073/pnas.1818604116>.
88. Robin S, Aresé M, Forte E, Sarti P, Giuffrè A, Soulimane T. A Sulfite Respiration Pathway from *Thermus thermophilus* and the Key Role of Newly Identified Cytochrome c550. J Bacteriol. 2011;193(15):3988–97. <https://doi.org/10.1128/jb.05186-11>.
89. Yu Z, Lemongello D, Segel IH, Fisher AJ. Crystal Structure of Saccharomyces cerevisiae 3'-Phosphoadenosine-5'-phosphosulfate Reductase Complexed with Adenosine 3',5'-Bisphosphate. Biochemistry. 2008;47(48):12777–86. <https://doi.org/10.1021/bi801118f>.
90. Matsuzawa T, Watanabe A, Shintani T, Gomi K, Yaoi K. Enzymatic degradation of xyloglucans by *Aspergillus* species: a comparative view of the genus. Appl Microbiol Biotechnol. 2021;105(7):2701–11. <https://doi.org/10.1007/s00253-021-11236-8>.

91. Backlund AE, Higgins MA. Identification and analysis of a unique group of glycoside hydrolase family 188 sequences with an altered sulfonate binding residue. *MicroPubl Biol*. 2024. <https://doi.org/10.17912/micropub.biology.001303>.
92. Guo SB, Wang MD, Xu W, Zou FX, Lin JJ, Peng Q, et al. Rapid screening of glycosyltransferases in plants using a linear DNA expression template based cell-free transcription-translation system. *Phytochemistry*. 2022;193. <https://doi.org/10.1016/j.phytochem.2021.113007>.
93. Martínez-Fleites C, Proctor M, Roberts S, Bolam DN, Gilbert HJ, Davies GJ. Insights into the Synthesis of Lipopolysaccharide and Antibiotics through the Structures of Two Retaining Glycosyltransferases from Family GT4. *Cell Chem Biol*. 2006;13(11):1143–52. <https://doi.org/10.1016/j.chembiol.2006.09.005>.
94. Chen B, Liu G, Chen Q, Wang H, Liu L, Tang K. Discovery of a novel marine *Bacteroidetes* with a rich repertoire of carbohydrate-active enzymes. *Comput Struct Biotechnol J*. 2024;23:406–16. <https://doi.org/10.1016/j.csbj.2023.12.025>.
95. Davies GJ, Gloster TM, Henrissat B. Recent structural insights into the expanding world of carbohydrate-active enzymes. *Curr Opin Struct Biol*. 2005;15(6):637–45. <https://doi.org/10.1016/j.sbi.2005.10.008>.
96. Armendáriz-Ruiz M, Rodríguez-González JA, Camacho-Ruiz RM, Mateos-Díaz JC. Carbohydrate esterases: An overview. *Methods Mol. Biol*. 2018;39–68. [https://doi.org/10.1007/978-1-4939-8672-9\\_2](https://doi.org/10.1007/978-1-4939-8672-9_2).
97. Mohammed ASA, Naveed M, Jost N. Polysaccharides; Classification, Chemical Properties, and Future Perspective Applications in Fields of Pharmacology and Biological Medicine (A Review of Current Applications and Upcoming Potentialities). *J Polym Environ*. 2021;29(8):2359–71. <https://doi.org/10.1007/s10924-021-02052-2>.
98. Nakamura AM, Nascimento AS, Polikarpov I. Structural diversity of carbohydrate esterases. *Biotechnology Research and Innovation*. 2017;1(1):35–51. <https://doi.org/10.1016/j.biori.2017.02.001>.
99. Nakamura T, Yonezawa Y, Tsuchiya Y, Niiyama M, Ida K, Oshima M, et al. Substrate recognition of N, N'-diacetylchitobiose deacetylase from *Pyrococcus horikoshii*. *J Struct Biol*. 2016;195(3):286–93. <https://doi.org/10.1016/j.jbsb.2016.07.015>.
100. Boraston AB, Bolam DN, Gilbert HJ, Davies GJ. Carbohydrate-binding modules: Fine-tuning polysaccharide recognition. *Biochem J*. 2004;382(3):769–81. <https://doi.org/10.1042/BJ20040892>.
101. Notenboom V, Boraston AB, Kilburn DG, Rose DR. Crystal structures of the family 9 carbohydrate-binding module from *Thermotoga maritima* xylanase 10A in native and ligand-bound forms. *Biochemistry*. 2001;40(21):6248–56. <https://doi.org/10.1021/bi0101704>.
102. Lombard V, Bernard T, Rancurel C, Brumer H, Coutinho PM, et al. A hierarchical classification of polysaccharide lyases for glycogenomics. *Biochem J*. 2010;432(3):437–44. <https://doi.org/10.1042/BJ20101185>.
103. Mathieu S, Henrissat B, Labre F, Skjåk-Bræk G, Helbert W. Functional Exploration of the Polysaccharide Lyase Family PL6. *PLoS ONE*. 2016;11(7). <https://doi.org/10.1371/journal.pone.0159415>.
104. Hobbs JK, Boraston AB. The structure of a pectin-active family 1 polysaccharide lyase from the marine bacterium *Pseudoalteromonas fuliginea*. *Acta Crystallographica Section F-structural Biology Communications*. 2024;80:142–7. <https://doi.org/10.1107/S2053230X2400596X>.
105. Buchan A, LeClerc GR, Gulvik CA, González JM. Master recyclers: features and functions of bacteria associated with phytoplankton blooms. *Nat Rev Microbiol*. 2014;12(10):686–98. <https://doi.org/10.1038/nrmicro3326>.
106. Sützl L, Laurent CVFP, Abrera AT, Schütz G, Ludwig R, Haltrich D. Multiplicity of enzymatic functions in the CAZy AA3 family. *Appl Microbiol Biotechnol*. 2018;102(6):2477–92. <https://doi.org/10.1007/s00253-018-8784-0>.
107. Lai Shi Min S, Liew SY, Chear NJ, Goh BH, Tan WN, Khaw KY. Plant Terpenoids as the Promising Source of Cholinesterase Inhibitors for Anti-AD Therapy. *Biology*. 2022;11(2). <https://doi.org/10.3390/biology11020307>.
108. Iliev I, Yahubyan G, Apostolova-Kuzova E, Gozmanova M, Mollova D, Iliev I, et al. Characterization and Probiotic Potential of *Levilactobacillus brevis* DPL5: A Novel Strain Isolated from Human Breast Milk with Antimicrobial Properties Against Biofilm-Forming *Staphylococcus aureus*. *Microorganisms*. 2025;13(1). <https://doi.org/10.3390/microorganisms13010160>.
109. Kahlke T, Goesmann A, Hjerde E, Willassen NP, Haugen P. Unique core genomes of the bacterial family vibronaceae: insights into niche adaptation and speciation. *BMC Genomics*. 2012;13. <https://doi.org/10.1186/1471-2164-13-179>.

## Publisher's Note

Springer Nature remains neutral with regard to jurisdictional claims in published maps and institutional affiliations.